A THREE PHASE AC-DC POWER TRANSISTOR CONVERTER CONTROLLED SEPARATELY EXCITED DC MOTOR DRIVE

by

SUSHIL KUMAR MANDAL

DEPARTMENT OF ELECTRICAL ENGINEERING
INDIAN INSTITUTE OF TECHNOLOGY, KANPUR

JULY, 1985

A THREE PHASE AC-DC POWER TRANSISTOR CONVERTER CONTROLLED SEPARATELY EXCITED DC MOTOR DRIVE

A Thesis Submitted
In Partial Fulfilment of the Requirements
for the Degree of

MASTER OF TECHNOLOGY

by
SUSHIL KUMAR MANDAL

to the

DEPARTMENT OF ELECTRICAL ENGINEERING
INDIAN INSTITUTE OF TECHNOLOGY, KANPUR
JULY, 1985

IN MEMORY OF MY MOTHER

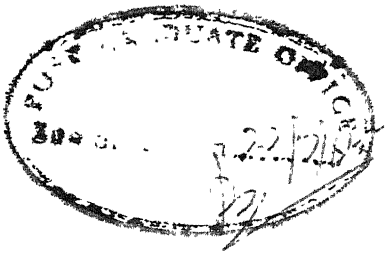

CERTIFICATE

This is to certify that the work on 'A THREE-PHASE AC-DC POWER TRANSISTOR CONVERTER CONTROLLED SEPARATELY EXCITED DC MOTOR DRIVE' by S.K. Mandal has been carried out under my supervision and this has not been submitted elsewhere for a degree.

July, 1985.

(S.R. DORADLA)
Assistant Professor
Department of Electrical Engineering
Indian Insitute of Technology
Kanpur-208016

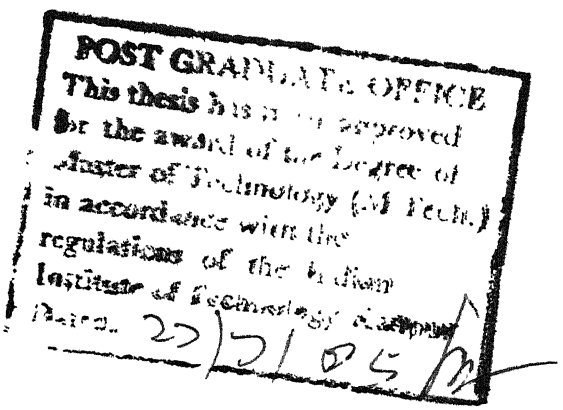

ACKNOWLEDGEMENTS

I would like to thank my thesis supervisor Dr. S.R. Doradla for his guidance and help throughout the project.

I wish to thank Mr. S.N. Sikdar for making available the power transistors without which this project could not have been completed.

I would like to thank Dr. A. Mahanta for taking the photographs presented in this thesis.

My thanks to Mr. S.N. Kole, Ramsingh of PCB Lab. and DVSSN Murthy, incharge of ACES workshop for his help of making power module in my project.

Finally to my friends, I express my thanks for their pleasant company at I.I.T. Kanpur.

Last, but not the least, I thank Mr. Yogendra for his neat and timely typing.

Sushil Kumar Mandal

IIT Kanpur

CONTENTS

LIST OF FIGURES

ABSTRACT

A static power converter is proposed using power transistors. The converter is potentially suitable for the speed control of a dc motor and static variable dc power supply as well. Considerable simplification has resulted by the use of power transistors since no commutation circuitry is required. Equal pulsewidth modulation(EPWM) control technique is employed for the static converter. The external performance characteristics of a three-phase ac-dc EPWM power transistor converter controlled separately excited dc motor are obtained for different speeds and modulating indexes without the filter in the input side of converter circuit. As the separately excited dc motors with the armature voltage control provide a constant torque operation the external performance characteristics are also obtained for this mode of operation. The effect of filters in the input side of the converter circuit is studied.

The power transistor converter has been built and the analytical results have been verified experimentally. The EPWM control has been implemented using a simple analog firing scheme. Eighteen pulses per half-cycle of the supply voltage have been selected since a band of lower order harmonics are

considerably reduced. The analysis of the supply current reveals that the predominant harmonic is seventeen times the supply frequency. This has a beneficial effect on the size of the input filter. The speed torque characteristics are obtained experimentally. The theoretical and experimental results are in good agreement. Experimental oscillograms of typical variables of the power transistor converter-motor system are illustrated to verify the basic principles of operation. The converter may find application in industrial drives employing dc motors and also in static variable dc power supplies.

CHAPTER 1

INTRODUCTION

In industrial applications, variable speed drives play an important role and for which control of power input or output is required. By virtue of controlled converter, the control of power input or output can be achieved. In early sixties, variable speed drives using dc motors were commonly and extensively used in industry because of their versatile speed-torque characteristics. It is well known that separately excited dc motors provide constant torque by armature voltage control upto the rated speed and constant power output by field control beyond the rated speed. Thus large range of speed control can be achieved both below and above the rated speed of dc motor.

All these factors motivated research in variable speed dc drives employing several schemes of controlling output power. Many schemes of controlling output power have been developed for speed control of dc motors, of all such schemes, three phase ac-dc pulse modulated converter provided versatile characteristics. With the rapid development of semiconductor devices, cheaper and better devices are being made available

like power transistors and MOSFET'S. These power devices are fast switching devices. The converter circuit as well as the control circuit is being simplified because these power devices do not require any commutating circuitry. Keeping in view of these developments, the study of three phase ac-dc equal pulse width modulated power transistor converter fed separately excited dc shunt motor drive was taken up. In equal pulse width modulation technique, eighteen pulses per half cycle of supply voltage was taken up. It is a variable voltage drive, with output voltage being controlled by switching technique within the converter itself. This makes the firing circuit of the converter quite simple. This converter is fabricated and tested on a separately excited dc shunt motor. A detail performance analysis of three phase ac-dc equal pulse width modulated power transistor converter fed separately excited dc shunt motor with as well as without filter taken into account in the input side of the converter was done and compared with the experimental results.

Section 1.1 deals with the contents of the thesis work chapterwise.

1.1 ORGANIZATION OF THESIS

Chapter 2 contains a brief literature survey on PWM schemes, different kinds of modulating techniques and

their implementations and calculation of firing angles and extinction angles. Chapter 3 deals with the detailed description of converter with firing circuit, snubber circuit, isolated power supply design and the basic principle of operation. Chapter 4 deals with the performance analysis, results, discussions and illustrations of oscillograms of the converter fed separately excited dc shunt motor drive. Chapter 5 deals with some sort of paper work on closed loop control of converter with resistive load. Chapter 6 deals with the conclusion of work and further scope of work in future.

CHAPTER. 2

LITERATURE REVIEW

2.1 INTRODUCTION

A dc machine is basically a variable speed machine, with versatile speed-torque characteristics. The voltage across the armature terminals is controlled for speeds below the rated speed keeping the field flux at the rated value while for speeds beyond the rated speed, the field flux is reduced. The highest speed attainable by field flux control is limited owing to commutation problems as commutator sparking and consequent limitations on the life of brushes and commutators. Althogh dc machines are costilier, need regular maintenance due to the presence of brushes and commutators yet the cost of the controller for a dc drive is lesser than that of an ac drive and the speed control is far more simple than that of an ac drive.

In late 1940 and early 1950, electronic control brought about a significant improvement in dc drive system limited to low power ratings. With the rapid development of power semiconductor switches, there has been a significant improvement

in the development of a power modulation for the dc drive systems. The power converter employing phase delay angle control technique for converting alternating voltage to direct voltage has been well established. In phase angle controlled converters, the ac voltage is switched on at delayed phase angles to obtain reduced dc output voltage. The main drawbacks associated with such converters are : poor supply power factor at large phase angle delays; generation of significant amount of lower order harmonics currents in the ac supply line; ripple in the output current. Such converters are simple, less expesive, reliable and do not require any external commutating circuitry. Although semiconverters or half controlled converters provide better power factor than full converters yet the improvement is only marginal. Thus the operation with poor power factor is a major concern in variable speed drives and also in high power applications. In order to improve the power factor and supply waveforms, various methods have been reported in the literature [1] - [3] . All these schemes are based on line commutation which require special types of control strategies. The converters employing forced commutation have been developed to improve the power factor and supply current waveform. Schemes with one forced commutation as well as several forced commutations per half cycle have been reported in the literature. Examples

of the former schemes are the wellknown symmetrical angle and extinction angle control schemes. The symmetrical angle control scheme provides unity displacement factor while the extinction angle control scheme can make the displacement factor leading. The leading power factor may not be desirable in systems with high source inductance. The forced commutation based on multi-pulse control has several beneficial effects over a single pulse control [4] ,[5]. Some of these are : the harmonic spectrum in the supply current shifts from lower to higher order making the supply current almost sinusoidal; the output current becomes quite smooth.

In order to keep the displacement factor at unity, the supply voltage is switched symmetrically with respect to the peak of the supply voltage. Such a control technique is defined as the pulse width modulation (PWM). Whenever a reference signal is compared with a carrier signal to generate firing pulses to thyristors in the converter, the ratio of the peak amplitude of reference wave to the peak amplitude of modulating wave is termed as modulating index 'm'. The carrier signal is usually a triangular wave while the modulating signal can be of different wave shapes. Thus there are various modulation schemes depending upon the waveform of the modulating signal. Fig. 2.1 illustrates different pulse width modulation

a_1 b_1 a_2 b_2

(a) EQUAL PULSE MODULATION

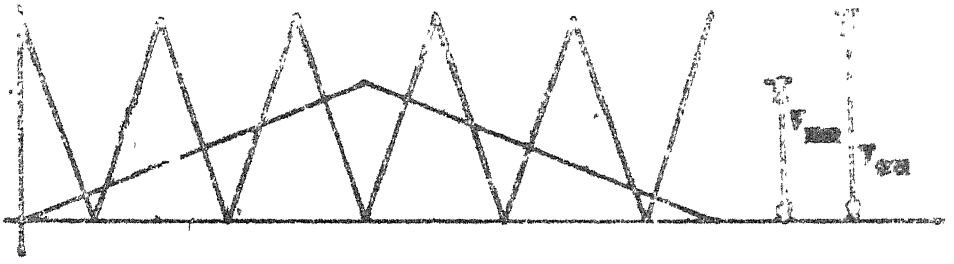

(b) TRIANGULAR PULSE MODULATION

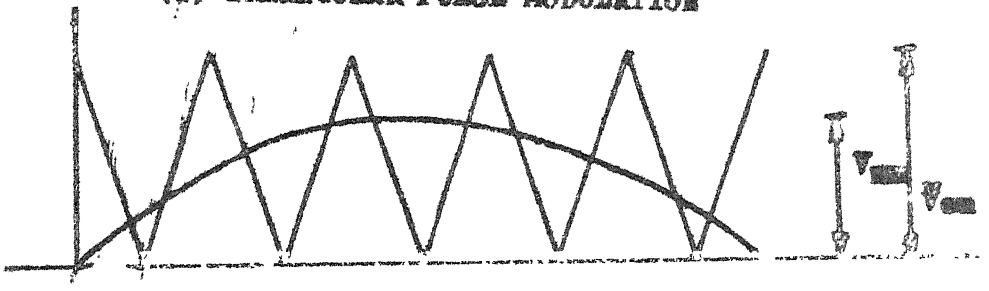

(c) SINUSOIDAL PULSE MODULATION

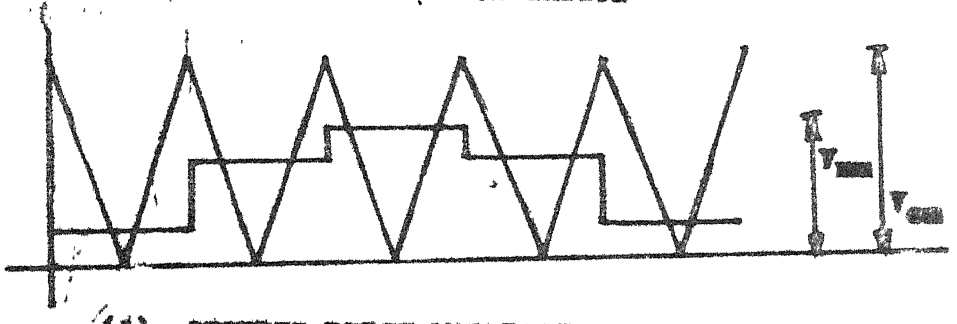

(d) STEPPED PULSE MODULATION

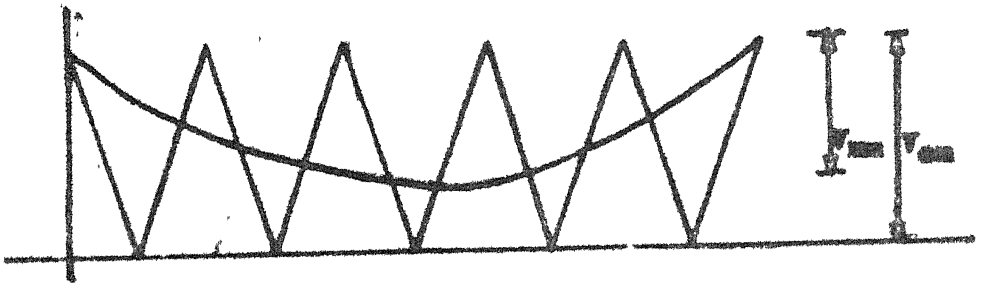

(e) INVERTED PULSE MODULATION

Fig. 2.1 Different Modulation Schemes

schemes. The output current and voltage waveforms depend on the type of modulation technique adopted. A comparative study of different modulation schemes has been reported on the basis of their external performances with R-L load [6]. It has been shown [6] , [10] that the inverted sine modulation as shown in Fig. 2.1(e) offers minimum ripple in the output current, minimum fundamental output voltage harmonics and maximum range of continuous conduction compared to other modulation schemes. In all modulation schemes, the output voltage range is limited except in the equal pulse width modulation (EPWM) where the output voltage variation is from zero to cent percent. Among all PWM techniques, the EPWM provides the maximum output voltage and offers better distortion factor without affecting the other performances significantly. Therefore the equal pulse width modulation technique (EPWM) as shown in Fig. 2.1(a) is employed for the converter proposed in this thesis.

The PWM techniques mentioned in the foregoing paragraphs are potentially suitable for the modern single phase AC traction where dc motors of large horsepower rating are supplied from single-phase AC supply systems via thyristorised converters. The improved performance is highly desirable in such applications. These techniques can also be applied to thyristorised dc drives used in various industries. Three-phase

converters are invariably used for medium and large power ratings. Since the conventional phase control technique deteriorates the performance, alternative control techniques are being actively considered for improving the performance [1] - [3] . These require special transformers but are still based on line commutation. The performance is also not improved significantly. For an improved performance, the forced commutation employing one of the PWM control technique is a must. There are a number of ways in which the forced commutation can be implemented [12] . A systematic study has been made in the configuration of ac-dc converters employing forced commutation [13] . A detailed study showing the supply performance and the load performance of an ac-dc converter-fed dc motor drive with SPWM control [14] . The converter circuit require some additional investment since it contains a few additional components in comparision with a line commutated three phase bridge converter. Because of forced commutation, the converter circuit undergoes several topological modes. The converter circuit if configured by power transistors or MOSFETS is greatly simplified. In.fact such converters because of their fast response are presently becoming a serious challenge to thyristor converters for output power rating upto 10-20 KW but where the power rating is more than 20KW thyristor converters are still preferred.

The advantages of power transistors and MOSFETS over thyristors are as follows:

i) Power transistors and MOSFETS can be turned 'on' and 'off' by the control of base and gate current.

ii) These devices can be operated at higher frequencies.

The disadvantages of power transistors and MOSFETS over thyristors are :

i) During on state, they have low transient overload capacity.

ii) The power dissipation capacity is low,

iii) At the present time, the rating is low.

iv) Their cost is higher and they are delicate to handle.

The power MOSFETS are ideal switches characterized by very high gain and extremely fast switching characteristics [8]. The presence of self capacitances in the device are nonlinear function of applied voltage and to some extent drain current. Under transient conditions, charging and discharging current flowing through those self capacitive elements makes the analysis of its characteristics during its operation more complex. Generally for convenience, these internal capacitive elements are assumed not to affect the transfer characteristics

between the gate voltage and the external drain current. Another reason is that users have rather an incomplete understanding of the MOSFET switching because these devices are still relatively new and the MOSFET circuit design know-how has not yet matured.

The objective is to study performance of a three-phase ac-dc converter using power transistors as switching elements, build the converter and verify its performance experimentally as well as theoretically with a separately excited dc shunt motor load. The effect of filters on the supply harmonic current is also studied.

2.2 CALCULATION OF FIRING AND EXTINCTION ANGLE :

As shown in Fig. 2.1a, the triangular signal v_c has been compared with a dc signal V_{mm}. The frequency of the triangular wave is 2p times the supply frequency, p being the number of pulses per half cycle. The modulating index is

$$m = \frac{V_{mm}}{V_{cm}}$$

α's, β's are considered as the firing and extinction angle respectively.

The firing angles α_k's and extinction angles β_k's are obtained by solving equations 2.1 and 2.2.

$$v_c(\alpha_k) - v_{mm}(\alpha_k) = 0 \qquad .. (2.1)$$

$$v_c(\beta_k) - v_{mm}(\beta_k) = 0 \qquad .. (2.2)$$

From equations 2.1 and 2.2, the firing angles and extinction angles in EPWM scheme are

$$\alpha_k = \frac{\pi(2k - 1 - m)}{2p} \qquad .. (2.3)$$

and $$\beta_k = \frac{\pi(2k - 1 + m)}{2p} \qquad .. (2.4)$$

where K = 1, 2, 3, ---- , p and α_k's, β_k's are in radians.

2.3 CONCLUSION

The operation of ac-dc power transistor converter, selection procedure for power transistors, design and fabrication of power circuit, firing circuit, snubber circuit, driver circuit and isolated dc power supplies are described in Chapter 3.

CHAPTER 3

AC-DC POWER TRANSISTOR CONVERTER-MOTOR SYSTEM EMPLOYING EQUAL PULSE WIDTH MODULATION CONTROL TECHNIQUE

3.1 INTRODUCTION

In this chapter, a simple three phase ac-dc converter circuit using power transistors is studied with a motor load. The converter employs EPWM control technique since it provides maximum output voltage besides improving other input and output performances. The complete ac-dc converter-motor system is described. The converter circuit configuration is given explaining the function of different elements that constitute the converter. The control circuit which produces the desired pulses for different power transistors is explained. The details of snubber circuit design, driver circuit and isolated dc power supply which are built in the laboratory are also included.

3.2 AC-DC POWER TRANSISTOR CONVERTER

The three phase ac-dc converter circuit using power transistors and suitable for implementing EPWM control technique is shown in Fig. 3.1. T_1-T_6 are power transistors

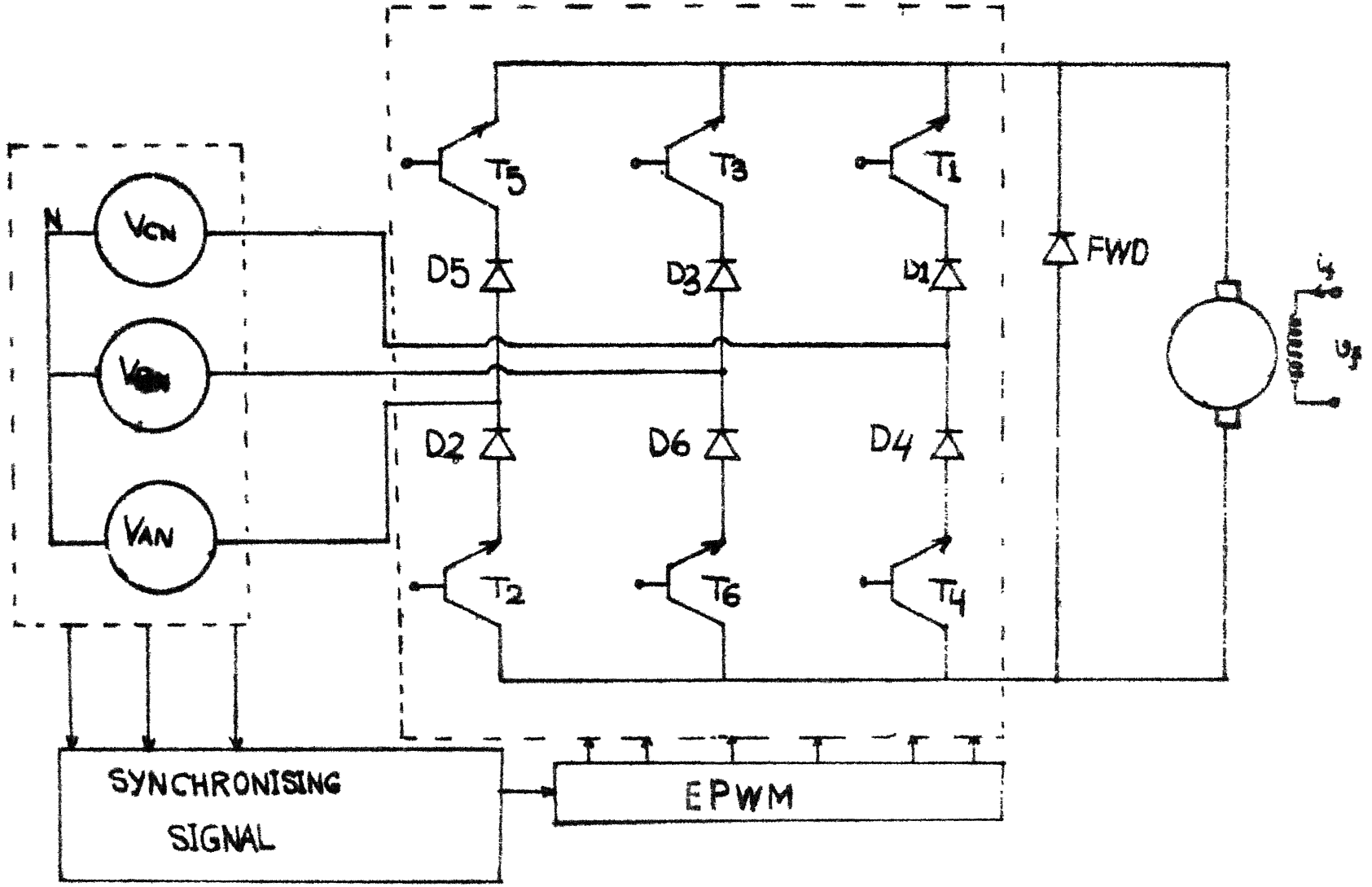

Fig 3.1 AC-DC POWER TRANSISTOR CONVERTER-MOTOR SYSTEM

which operate either in saturation mode or cut off mode depending upon whether base pulses are present or not. The necessary pulses conforming to EPWM control technique are generated in a control circuit. In the presence of diode D_1-D_6, power transistors do not experience any negative voltage of the supply which is undesirable in practice. T_1, T_3 and T_5 are turned on and off several times in each cycle of supply voltage, while T_2, T_4 and T_6 are given 120° continuous pulses during the positive half of the respective supply voltage only. The EPWM control technique employs eighteen pulses per half-cycle of each phase of the supply voltage. Each transistor conducts for 120° interval of supply voltage and at any instant two transistors one in the top group and the other in the bottom group conduct impressing appropriate line voltage across the output terminals. For example, if T_1 and T_6 conduct along with the diodes D_1 and D_6, the line voltage v_{AB} is impressed across the output terminals. The pairs of transistors that conduct are T_1T_6, T_1T_2, T_2T_3, T_3T_4, T_4T_5, T_5T_6 and the respective voltages are v_{AB}, v_{AC}, v_{BC}, v_{BA}, v_{CA}, v_{CB}. During the interval when the power source is switched off from the output terminals, the diode SWD conducts providing freewheeling path for the load current.

3.3 ANALOG FIRING SCHEME

The block diagram of the analog firing scheme for a three phase ac-dc converter suitable for any number of pulses per half cycle of the supply phase voltage is shown in Fig. 3.2(a). The firing circuit is designed for eighteen pulses per half cycle of supply phase voltage. The digital chip layout diagram is shown in Fig. 3.2(b).

In this section, the hardware realisation for the generation of switching pulses for transistors T_1 and T_4 is described. Switching pulses for other pairs of transistors T_3 and T_6, T_2 and T_5 are generated in the similar manner.

A synchronizing signal is obtained by stepping down the phase A voltage from 230V, 50Hz to 6V-0V-6V, 50Hz with the help of a single-phase transformer having 230V/6V-0V-6V, 1 Amp , 50Hz rating. The secondary output of the single-phase transformer having the signal across 6V-0V terminal is taken as the synchronising signal(s). The signal S is transformed into a square wave by a zero crossing detector using an operational amplifier. The square wave U is taken as the reference signal for the phase locked loop (PLL) using the chip, CD4046. The PLL in its feedback path (K1) has a 'devide by 2p' using two counters namely 7492 having a maximum count of

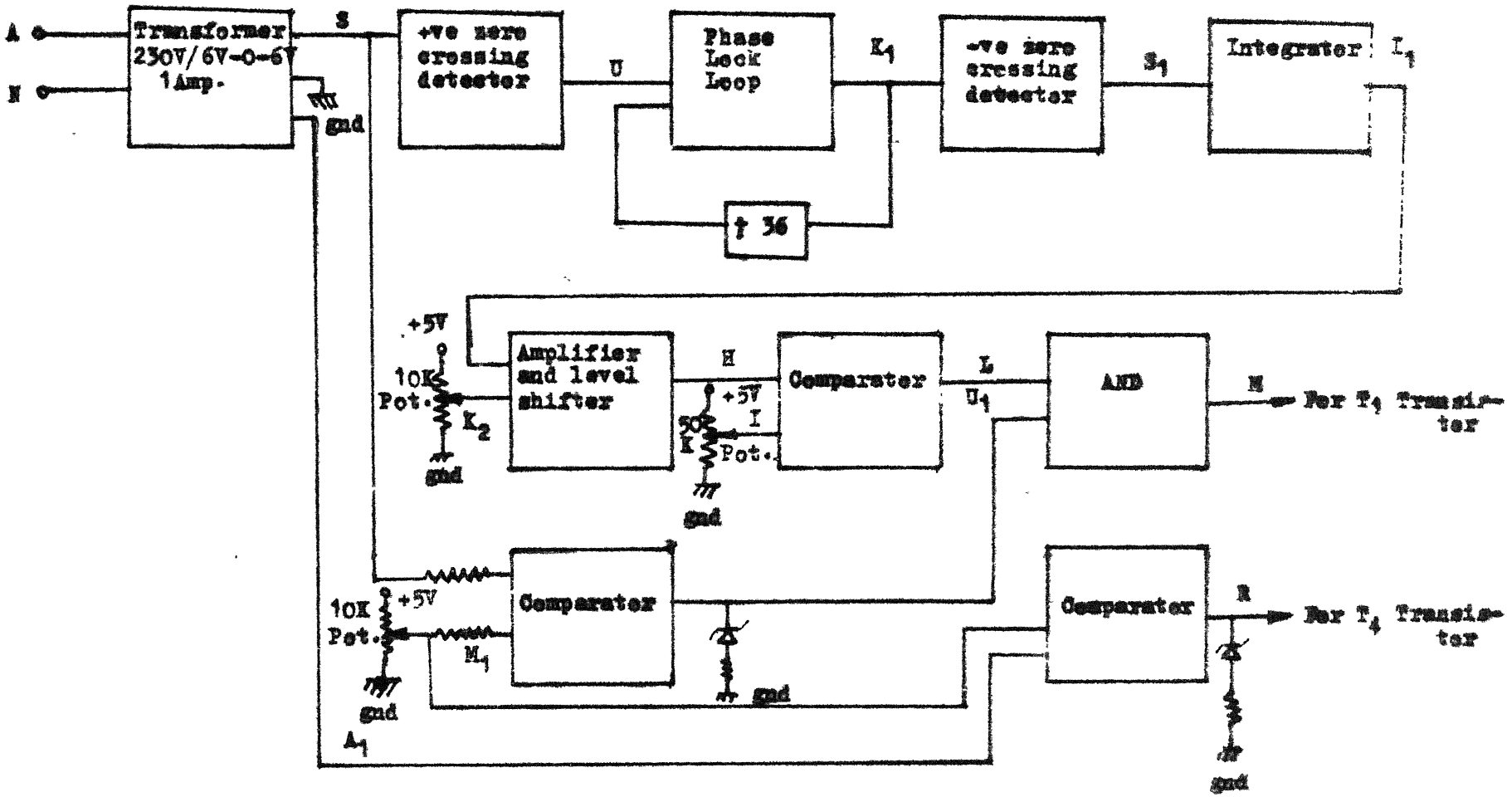

Fig. 3.2(a) BLOCK DIAGRAM FOR FIRING CIRCUIT

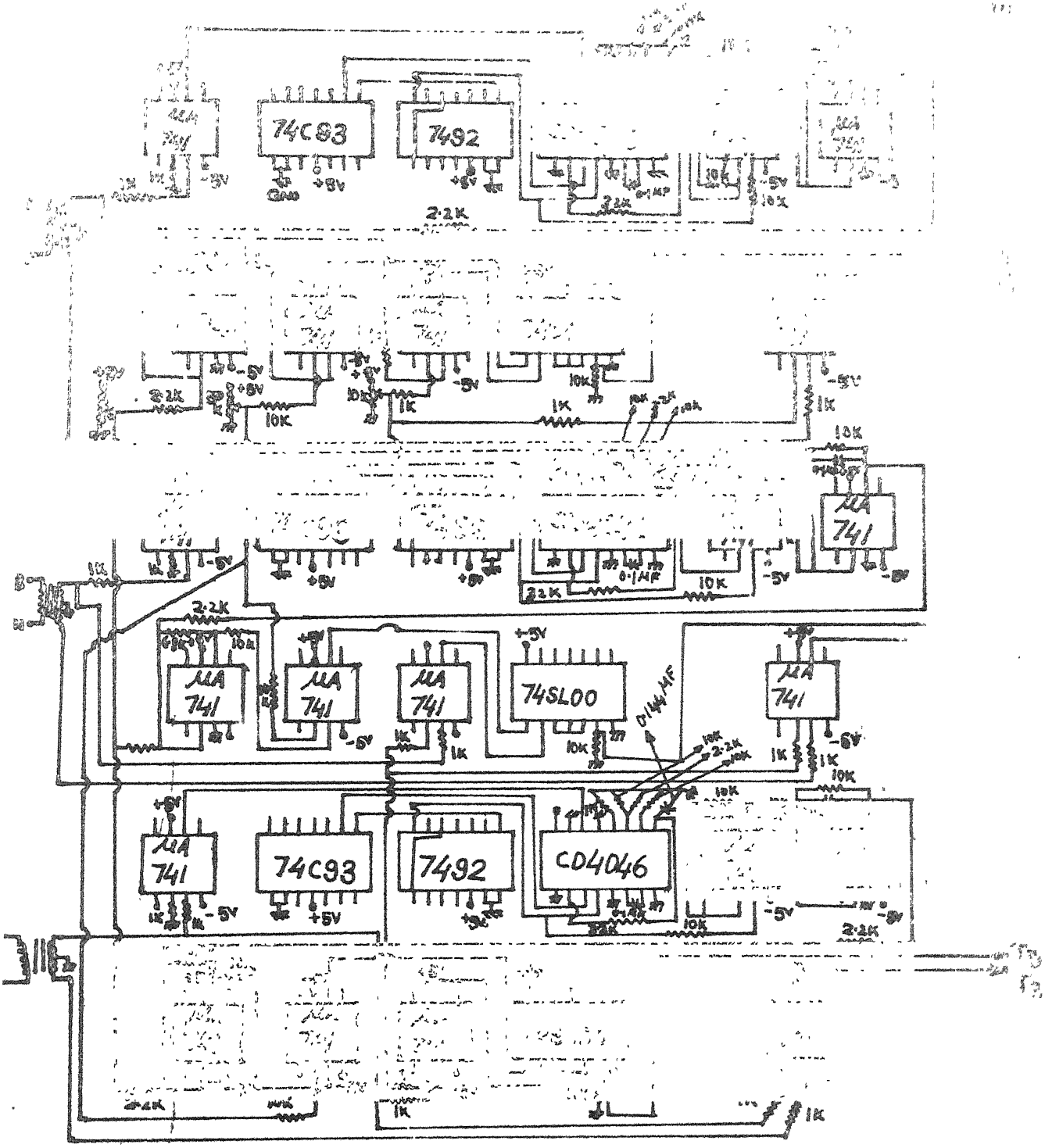

Fig. 5.4(a) PINOUT DIAGRAM

12 and 74C93 having a maximum count of 16, where p is the number of pulses per half of the supply phase voltage. The signal K1 is passed through a negative zero crossing detector using μA741 chip to obtain a ± 2.5V swing of a square wave S_1 having frequency equal to 2p times that of the synchronising frequency. The signal S_1 is now integrated using an active device (μA741 chip) to obtain a triangular wave I_1 having the swing ± 2.0V. The signal I_1 is now amplified and level shifted (by adding + 2.0V with the help of 10K potentiometer) using μA741 chip to obtain a triangular wave H having amplitude 0V and 5V. The signal H is now compared with a dc signal K2 using μA741 chip to obtain a square wave that is a train of square pulses. The dc signal K2 is varied from a 50kΩ potentiometer having smooth voltage variation ranging from 0 to + 5V in steps of 0.1V. As the signal K2 increases, the width of the square pulse increases. The signal K2 is the modulating signal and the signal H is the carrier signal having constant frequency and amplitude. As the modulating signal K2 is varied, this in turn varies the modulation index m.

The signal from the secondary output (6V-0V) terminals is compared with a dc signal M1 using 10K pot. and negative half of the comparator output has been clipped using a diode in series with a resistance in series to limit current through

the diode to obtain a 120^{o} pulse U_1. The signal L is anded with U_1 to obtain a discrete square pulse train M only during the 120^{o} interval of the positive half of the phase A which is symmetrical about the positive half of phase A . The firing pulse so generated is applied to power transistor T_1.

The signal A_1 from the secondary output of single phase transformer (OV-6V) terminals is compared with signal M_1 and the negative half of the comparator output have been clipped using a diode in series with a resistance to limit the current through diode to obtain a 120^{o} pulse R. This firing pulse generated is applied to power transistor T_4. For the generation of firing pulses for other two pairs of transistors (T_3, T_6 and T_5, T_2), the level shifting signal K2, signal I, signal M_1 is taken as the common signal but the synchronising signal for the generation of firing pulses for pair of transistors (T_3, T_6) is drawn from phase B and that of pair (T_5,T_2) from phase C by stepping down as obtained for T_1, T_4 transistors. The waveforms in each stage for the generation of control pulses for transistors T_1 and T_4 are shown in Fig. 3.2(c). Control pulses for transistors T_1 to T_6 are shown in Fig.3.2(d).

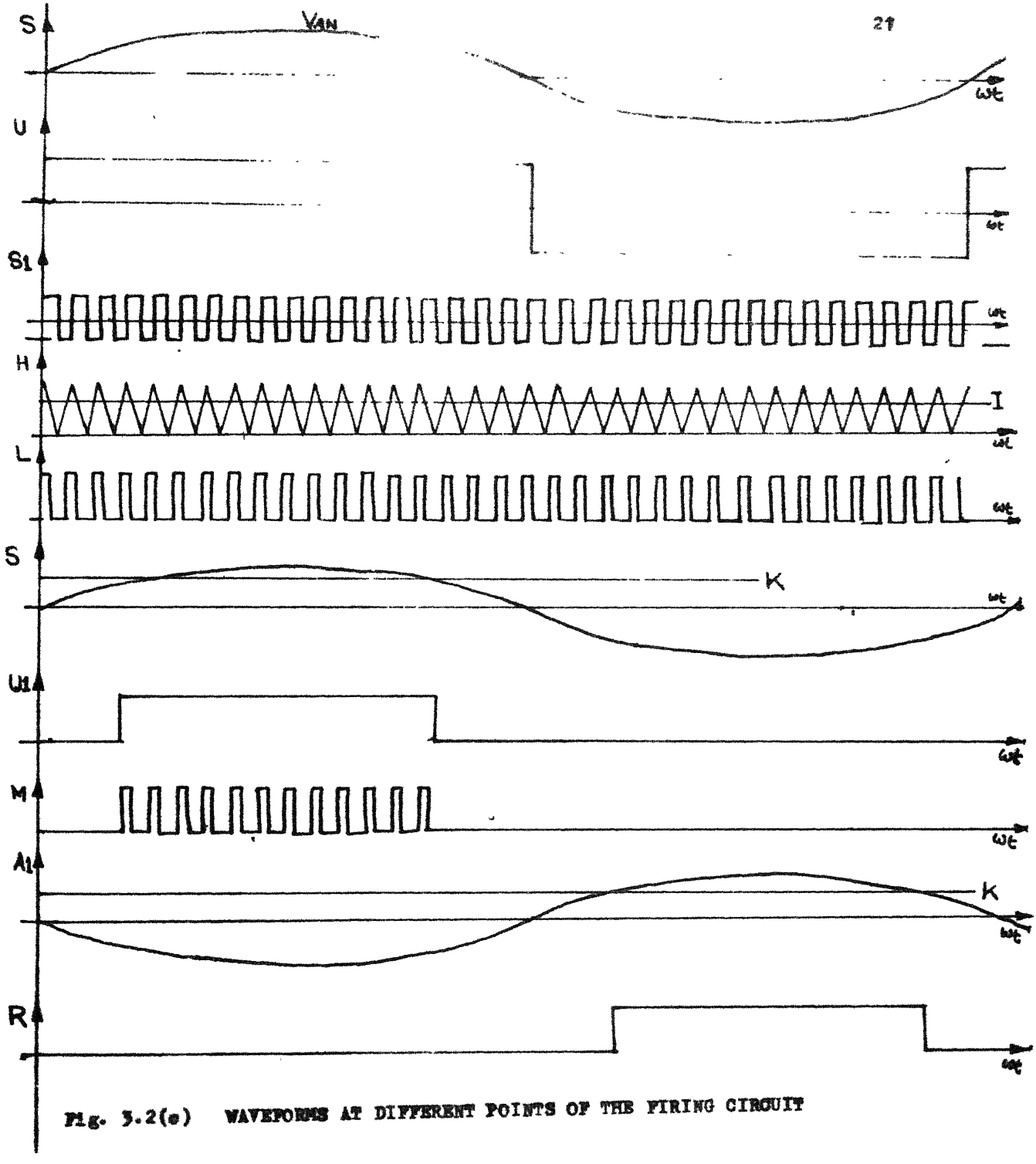

Fig. 3.2(e) WAVEFORMS AT DIFFERENT POINTS OF THE FIRING CIRCUIT

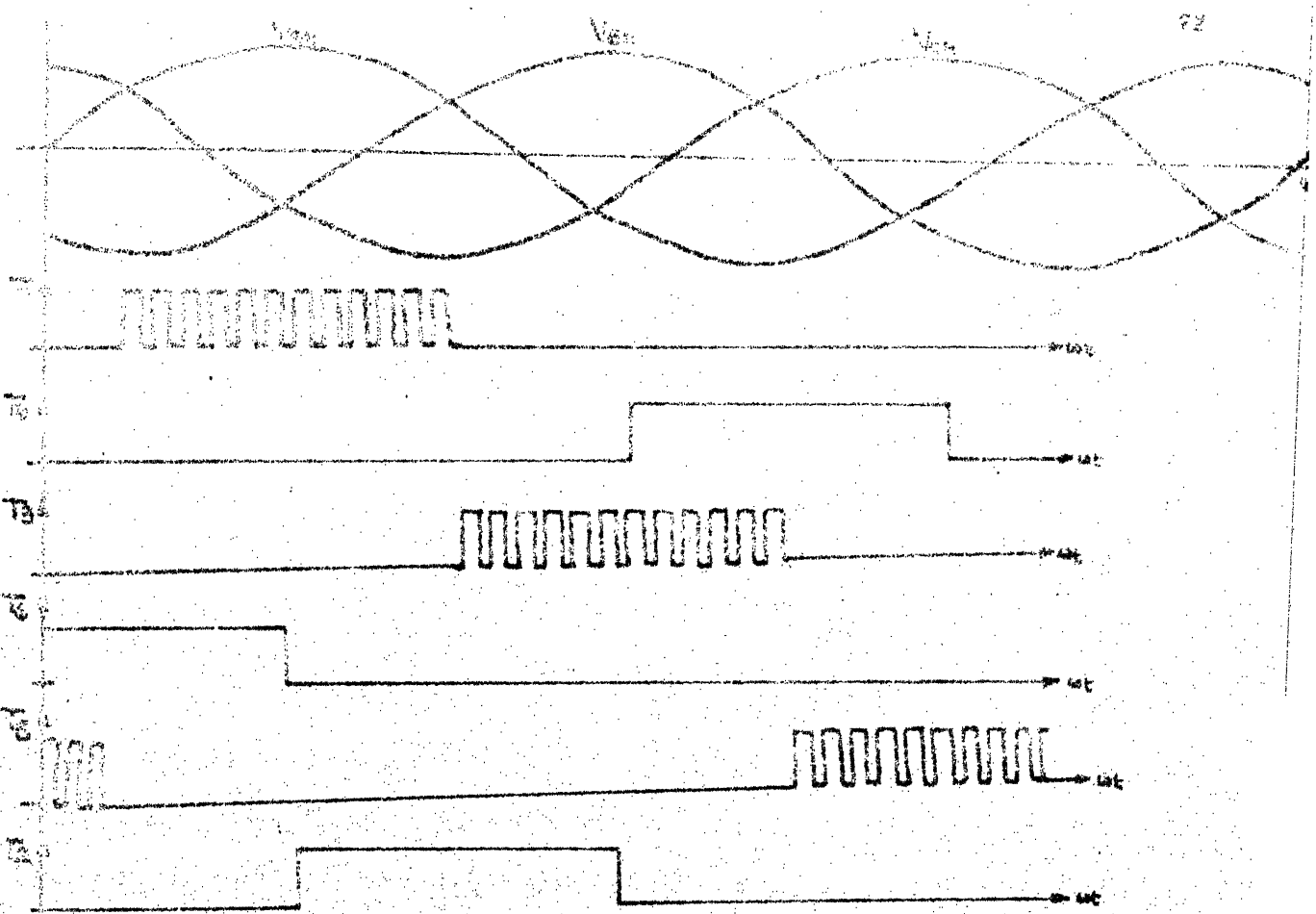

Fig. 3.2(c) FIRING PULSES FOR THE POWER TRANSISTORS IN THE CONVERTER CIRCUIT

3.4 SELECTION OF DEVICES

Each transistor in the converter of Fig. 3.1 is realized by a power darlington MJ10009. The internal circuit details of MJ10009 are shown in Fig. 3.3. The maximum current and voltage ratings of the device are 30A and 600V respectively. It has low base drive requirement because of darlington construction. In the internal circuit of this power transistor, the speed-up diode helps faster turn off and the fast recovery rectifier between collector and emitter can eliminate the need for an external diode to clamp inductive loads. Rating of MJ10009 is given in Appendix B.

3.5 SNUBBER CIRCUIT DESIGN

While designing the snubber circuit for any power transistor, the specified operating area as well as the reverse bias safe operating area (RBSOA) during turn off time of power transistor should be taken into account because the presence of invariable stray inductance in the circuit produces an overshoot in the collector voltage, when the power transistor is being turned off. So the purpose of the snubber circuit is to restrict the operating point within this RBSOA. Fig. 3.4(a) shows the RBSOA of MJ10009 and Fig. 3.4(b) shows the snubber circuit designed for power transistor MJ10009. The

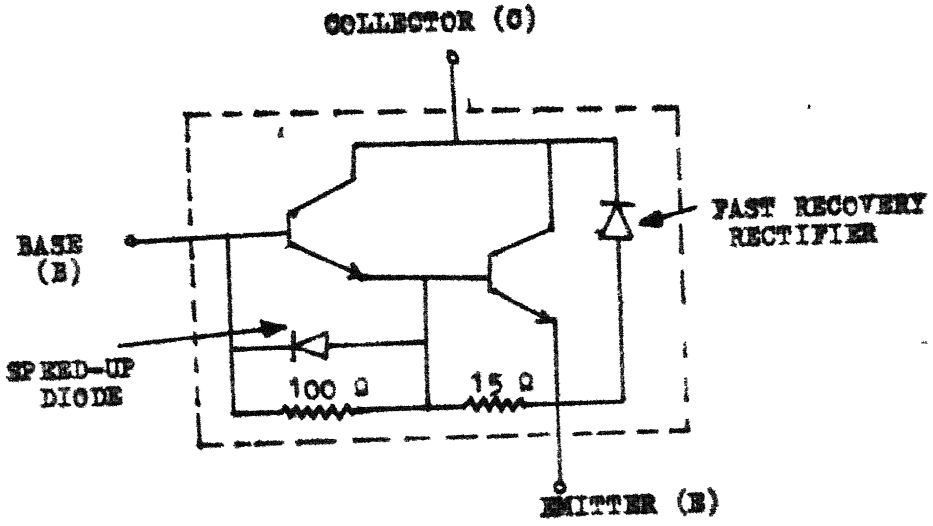

Fig. 3.3 MJ10009 INTERNAL CONFIGURATION

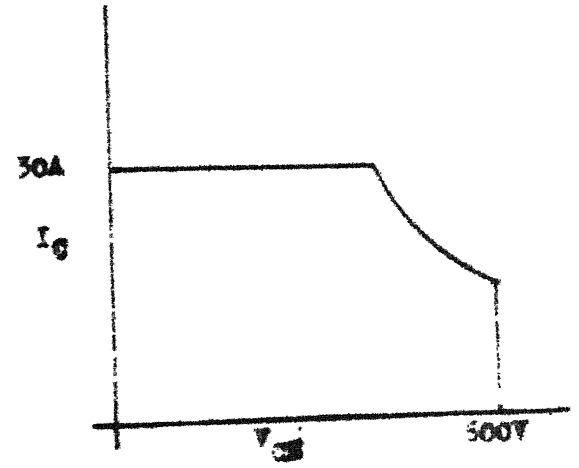

Fig. 3.4(a) RBSOA OF MJ10009

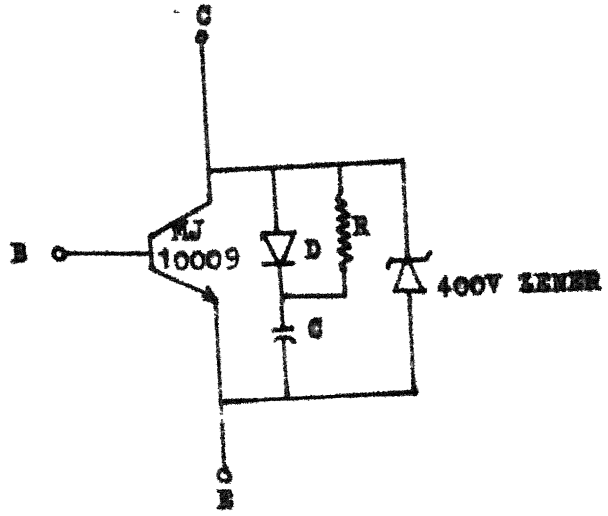

Fig. 3.4(b) SNUBBER CIRCUIT

snubber circuit design [11] is adopted with some modifications. A zener diode has been inserted between collector and emitter in order to maintain the collector voltage within some safe value according to the specifications given for power transistor MJ10009. The value of snubber capacitor is given by

$$C = \frac{I_c t_m}{V_Z}$$

I_c = Maximum collector current of MJ10009 = 30A

V_Z = Zener Voltage = 400V

t_m = Minimum turn off time = 1.8μsec.

$$C = \frac{30 \times 1.8 \times 10^{-6}}{400} = 0.1\ \mu F$$

Here RC = Minimum on time

As minimum on tine = 10 μSec. RC = 10μsec.

$$R = \frac{10 \times 10^{-6}}{0.1 \times 10^{-6}}\ \Omega = 100\ \Omega$$

As the switching pulse frequency f_{max} = 1.8 KHz

Power loss P_R in R is given by

$$PR = \frac{1}{2} C V_Z^2 f_{max} = \frac{1}{2} \times 0.1 \times 10^{-6} \times (400)^2 \times 1.8 \times 10^3 = 14 \text{ watts.}$$

Designed values are R = 100 Ω , 14 watts and C = 0.1 μF

3.6 DRIVER CIRCUIT

The firing pulses for transistors T_1 to T_6 as obtained from the control circuit do not fulful the requirements of base drive for the MJ10009 transistors. It is necessary to design the driver circuit for fulfilling the requirement of base drive for MJ10009 type transistors. The driver circuit is designed for a collector current of 10 Amps for which the minimum h_{fe} is 40 as shown in Fig. 3.5 [15]. The power transistors require a base drive of 250mA but with an overdrive factor of 2.4, a base drive of 600mA has been provided using the transistor SL100. With this overdriving of the base, the operation of the transistor MJ10009 in the transient condition will be reliable and will reduce the steady state loss due to reduction in V_{CE} (sat). In the output side, the push pull configuration is given using SL100 and SK100. The function of SL100 and SK100 is to keep them active during the on and off periods of MJ10009 respectively. This helps in reducing the turn-off of transistor MJ10009, by removing the base stored charge. The capacitors across the collector of SL100 and SK100 improve the switching.

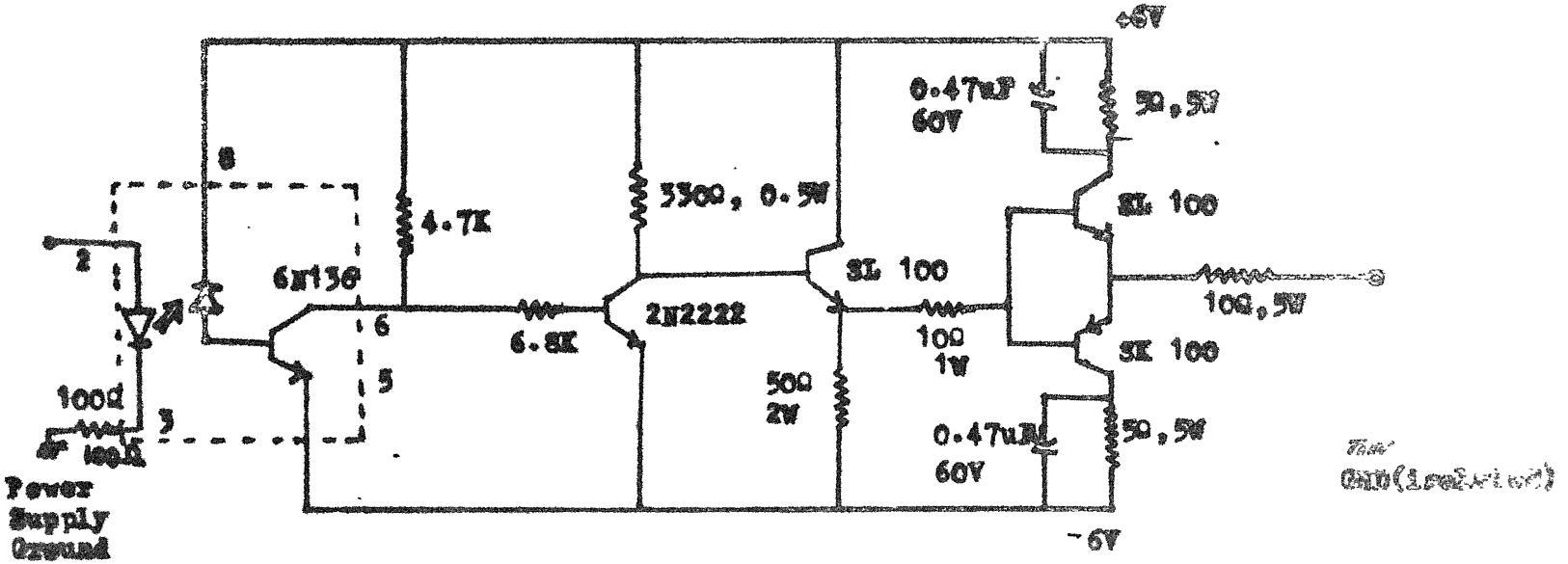

Fig. 3.5 DRIVER CIRCUIT

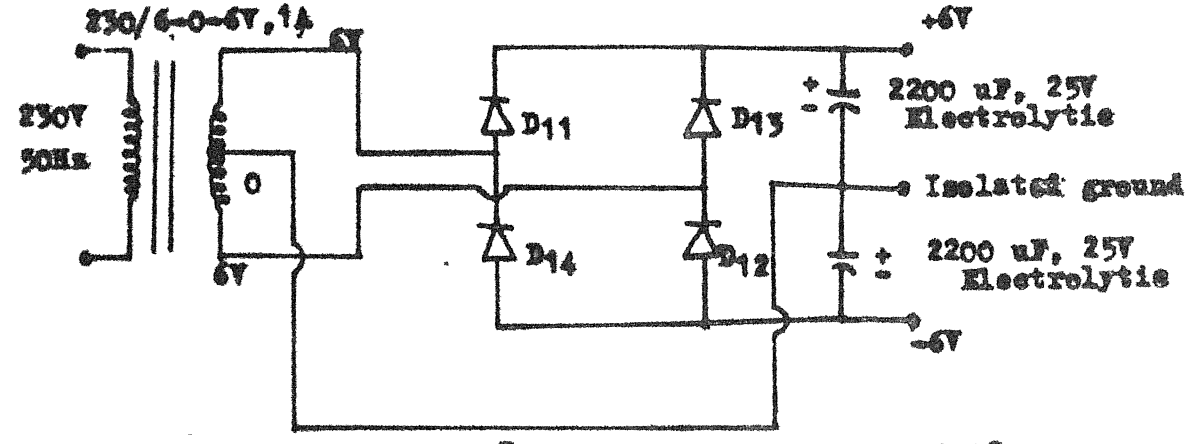

D_{11}, D_{12}, D_{13}, D_{14} - Diode IN4002

Fig. 3.6 ISOLATED POWER SUPPLY

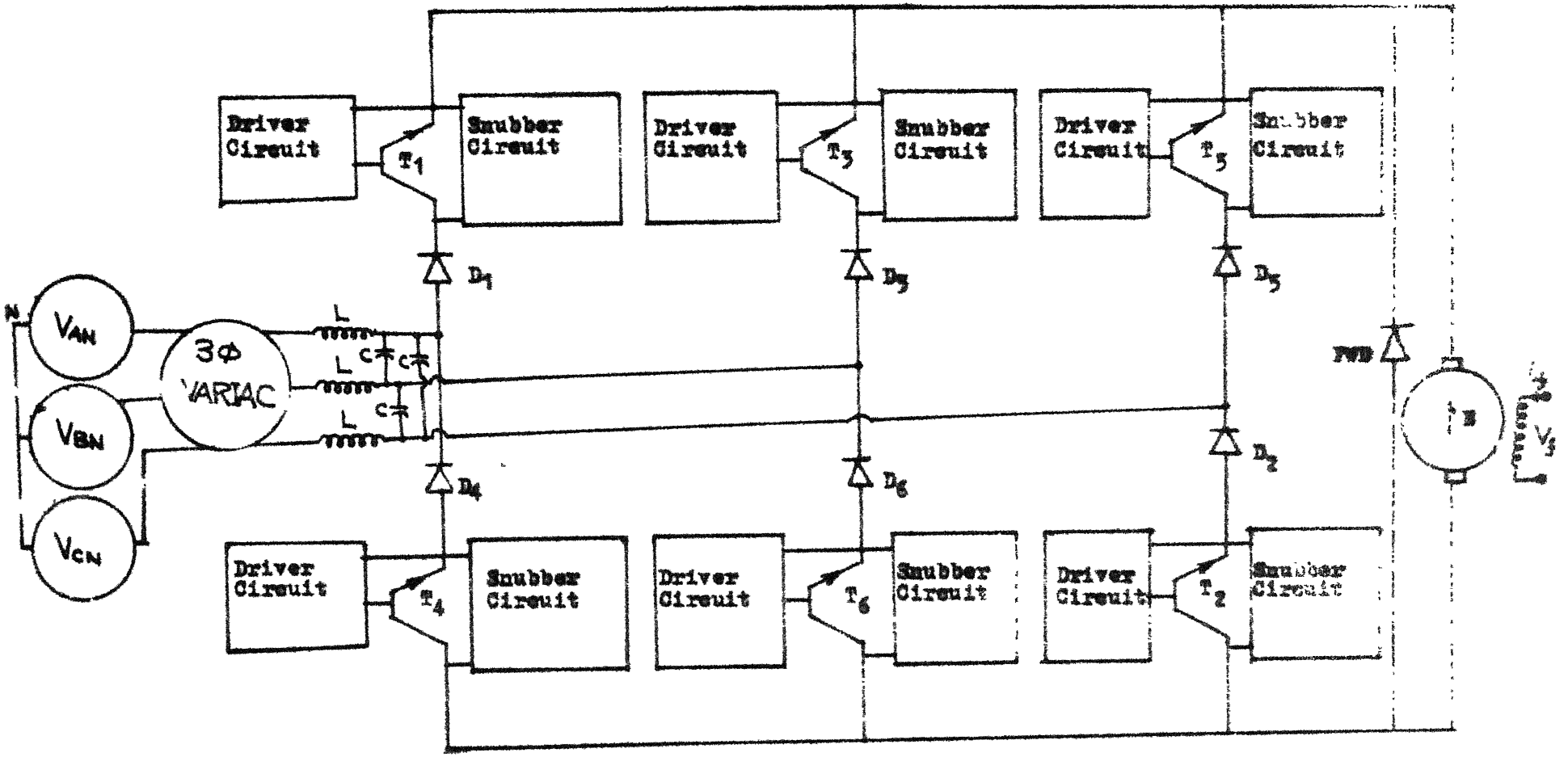

Fig. 3.7 EXPERIMENTAL SETUP

3.7 ISOLATED POWER SUPPLY

The isolated dc power supply as shown in Fig. 3.6 for each driver circuit required for each power transistor has been designed for the converter circuit. The isolated dc power supply ratings are ± 6 Volts and 1 amp each. It has been designed with a full wave diode bridge using IN4002 diode with capacitor filter. The complete experimental setup is shown in Fig.3.7. The rating of motor is given in Appendix A.

3.8 CONCLUSION

In the next chapter, the performance analysis and characteristics have been discussed for the three-phase AC-DC power transistor converter fed separately excited dc motor drive. The performance is studied both with and without filters.

CHAPTER 4

STEADY STATE PERFORMANCE CHARACTERISTICS

4.1 INTRODUCTION

In this chapter, the input and output characteristics of a three phase ac-dc power transistor converter controlled dc separately excited motor are throughly investigated with the motor running under motoring mode of operation. The supply performances consists of power factor, displacement factor, harmonic factor, distortion factor and supply harmonic spectra, while the load performances are evaluated in terms of ripple factor and peak factor. These are determined for different speeds and modulating indexes and also for constant torque operation of the motor. The effect of input filter on the performance characteristics is investigated. The speed-torque characteristics are also illustrated. The discrepancies between the theoretical and experimental results are alwo shown in this chapter.

4.2 PERFORMANCE CHARACTERISTICS WITHOUT INPUT FILTER

In this section, the analysis of output voltage and steady state output current waveforms is presented and the

converter circuit is assumed to operate according to equal pulse width modulation technique. As the output voltage repeats after six pulses as shown in Fig.4.1(a), it is sufficient to consider the current waveform for any six pulses if steady state performance is being derived. As the mechanical time constant is much more higher than the electrical time constant of the motor armature circuit, the speed fluctuations under steady state can be neglected. For a given value of modulating index 'm,' switching on and off angles are computed as explained in Chapter 2.

The output voltage waveform v_o of the converter is shown in Fig. 4.1(a). The average value of output voltage will be

$$V_{dc} = \frac{1}{\pi/3} \int_{\pi/3}^{\pi/2} v_{AB}\, d\theta = \frac{3}{\pi} \int_{\pi/3}^{\pi/2} 3\sqrt{6}\, E_{ph} \sin(\theta + \pi_6)\, d\theta$$

As $v_{AB} = 3\sqrt{6}\, E_{ph} \sin(\theta + \pi/6)$

$$V_{dc} = \frac{3\sqrt{6}\, E_{ph}}{\pi} \int_{\pi/3}^{\pi/2} \sin(\theta+\tfrac{\pi}{6})\, d\theta = \frac{3\sqrt{6}}{\pi} E_{ph} \cos(\beta_1+\tfrac{\pi}{6})$$

$$- \cos(\alpha_1 + \tfrac{\pi}{6}) + \text{----} + \cos(\beta_6+\tfrac{\pi}{6}) - \cos(\alpha_6+\tfrac{\pi}{6})$$

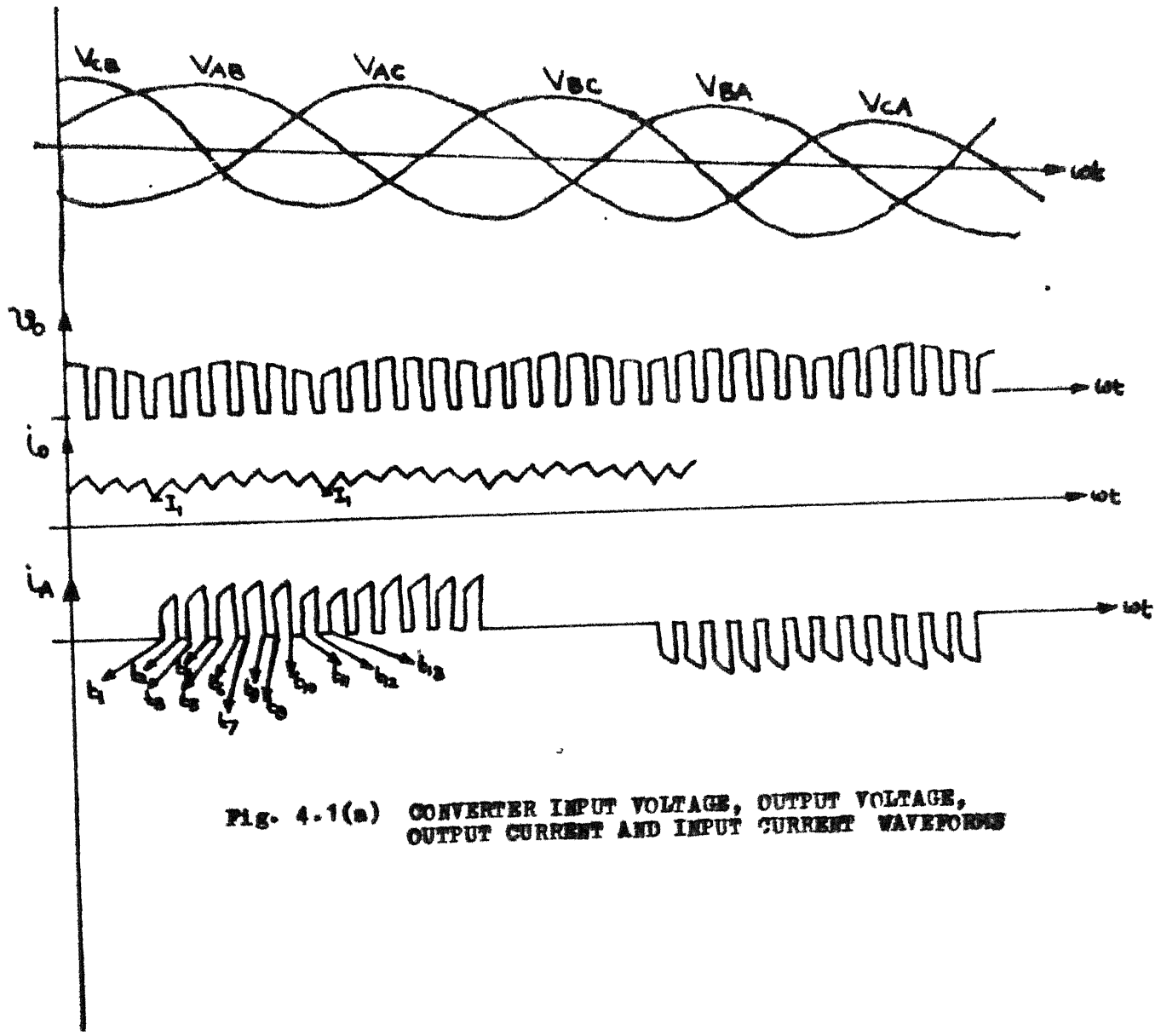

Fig. 4.1(a) CONVERTER INPUT VOLTAGE, OUTPUT VOLTAGE, OUTPUT CURRENT AND INPUT CURRENT WAVEFORMS

So in a generalised way we can write the average voltage as follows :

$$V_{dc} = \frac{3\sqrt{6}\, E_{ph}}{\pi} \sum_{i=1}^{p/3} [\cos(\beta_i + \pi_6) - \cos(\alpha_i + \frac{\pi}{6})] \quad .. (4.1)$$

where p, α's and β's are the number of pulses per half cycle, switching on angles and switching off angles respectively.

α's and β's are being evaluated with the help of equations 2.3 and 2.4 respectively discussed in Chapter 2.

The relation between α's and β's with time is as follows :-

$$\alpha_i = w\, t_{2n+1} \; ; \quad \beta_i = w\, t_{2n+1}$$

where w = Angular frequency = 50 Hz; i = 1,2, ..., 6;

n = 0,1,2, ...,6.

The expression 4.1 shows that the average output voltage depends on number of pulses per half cycle, switching on and off angles.

Equation 2.3 and 2.4 shows that switching on and off angles depend on number of pulses per half cycle p and modulating index m. So it can be written,

$$v_{dc} = f(p, \alpha, \beta) = f(m)$$

The average output voltages V_s modulating index m shows a linear curve passing through origin. The theoretical relationship between output voltage and modulating index m is in well agreement with the practical one. It is shown in Fig. 4.1(b). The instantaneous output current is analysed and calculated over a period of 60^o starting from t_1 as shown in Fig. 4.1(a). The 60^o span of time consists of six power intervals and six freewheeling intervals. Let the voltage applied across the load during the interval $t_1 - t_{12}$ is v_{ab}. Let the steady-state instantaneous output current at $t_1, t_2, ---, t_{13}$ be denoted as $I_1, I_2, --, I_{13}$ respectively.

During the power interval, the governing instantaneous voltage equation is

$$E + L\frac{di_o}{dt} + Ri_o = \sqrt{6}\, E_{ph} \sin\left(wt + \frac{\pi}{6}\right)$$

where L = Total armature circuit inductance

R = Total armature circuit resistance

E = Motor Back e.m.f.

w = Angular frequency of the three phase ac supply=50Hz

E_{ph} = R.M.S. per phase supply voltage.

$$L\frac{di_o}{dt} + Ri_o = \sqrt{6}\, E_{ph} \sin\left(wt+\frac{\pi}{6}\right) - E \qquad \frac{di_o}{dt} + \frac{R}{L} i_o = \frac{3\sqrt{6}E_{ph}}{L} \sin\left(wt+\frac{\pi}{6}\right) - \frac{E}{L}$$

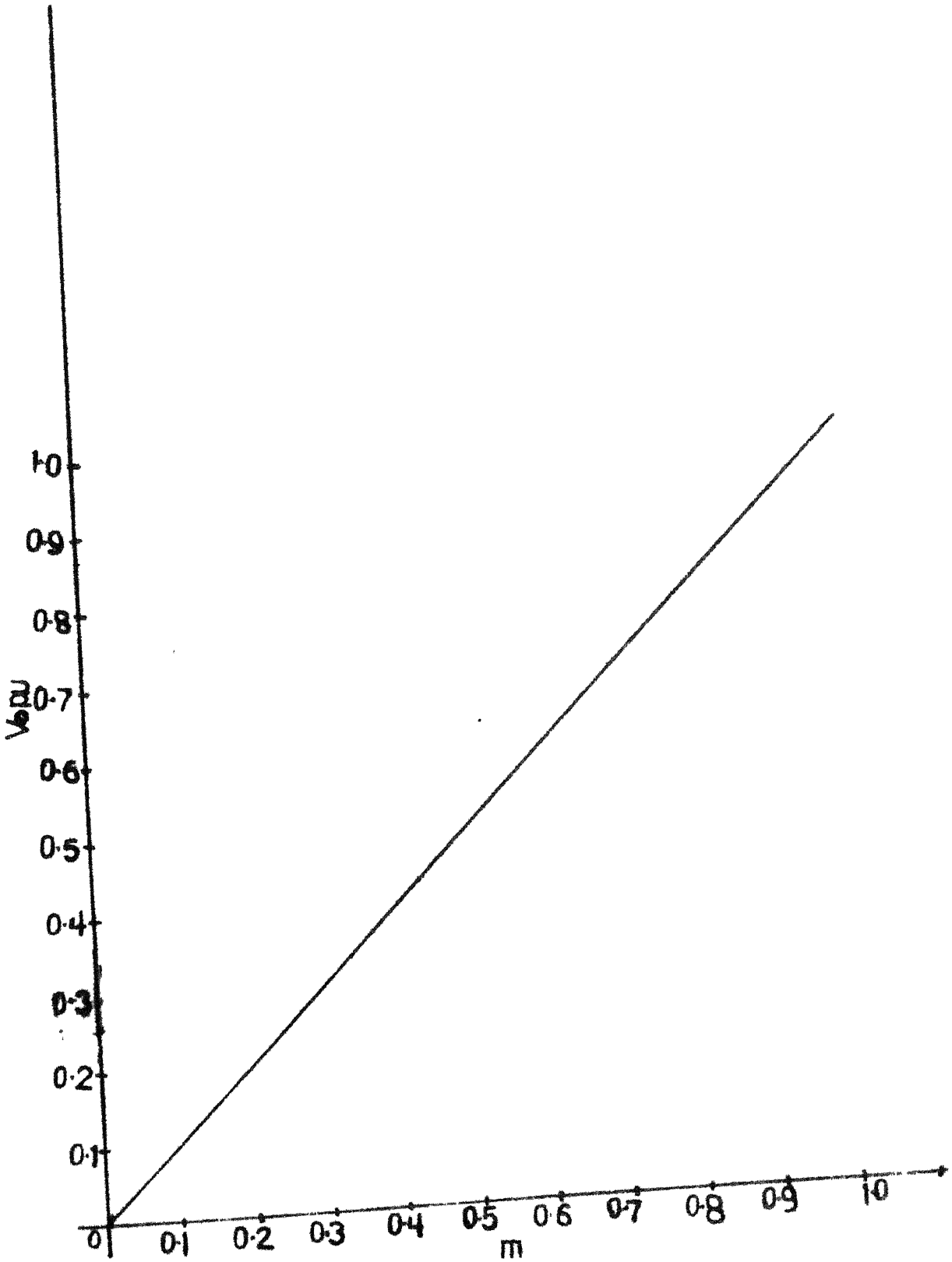

Fig 4.10 AVERAGE OUTPUT VOLTAGE VS MODULATING INDEX

So C.F. of differential equation will be $\frac{di_o}{dt} + \frac{R}{L} i_o = 0$.

Let $i_o = K e^{-mt}$

$\frac{di_o}{dt} = -K m e^{-mt}$ So $-K m e^{-mt} + \frac{R}{L} K e^{-mt} = 0$

$$m = \frac{R}{L} \quad [\text{As } K \neq 0 \; ; \; e^{-mt} \neq 0]$$

So $i_o = K e^{-Rt/L} = K e^{-t/(L/R)}$; Let $\frac{L}{R} \tau$ = motor time constant

So $i_o = K e^{-t/\tau}$ Here K is the constant, being evaluated from initial condition.

P.I of differential equation will be

$$P.I = \frac{1}{D+\frac{R}{L}} \left[\frac{\sqrt{6}\, E_{ph}}{L} \sin\left(wt+\frac{\pi}{6}\right) \right] - \frac{1}{D + \frac{R}{L}} \left(\frac{E}{L}\right)$$

$$= \frac{D - R/L}{D^2 - \frac{R^2}{L^2}} \left[\frac{\sqrt{6}\, E_{ph}}{L} \sin\left(wt + \frac{\pi}{6}\right) \right] - \frac{L}{R} \left[1 + D. \frac{R}{L}\right]^{-1} \left(\frac{E}{L}\right)$$

$$P.I = \frac{D-R/L}{-w^2 - \frac{R^2}{L^2}} \left[\frac{\sqrt{6}\, E_{ph}}{L} \sin\left(wt + \frac{\pi}{6}\right) \right] - \frac{E}{R}$$

$$= \frac{\sqrt{6}\, E_{ph}}{R^2 + w^2 L^2} \left[-wL \cos\left(wt + \frac{\pi}{6}\right) + R \sin\left(wt + \frac{\pi}{6}\right) \right] - \frac{E}{R}$$

$$P.1 = \frac{\sqrt{6}\, E_{ph}}{Z} \sin(wt + \frac{\pi}{6} - \varphi) - \frac{E}{R} \quad ;$$

where $Z = \sqrt{R^2 + w^2 L^2}$; $\varphi = \tan^{-1}(\frac{wL}{R})$

So instantaneous equation for the output current i_o will be

$$i_o = K\, e^{-t/\tau} + \frac{\sqrt{6}\, E_{ph}}{Z} \sin(wt + \frac{\pi}{6} - \varphi) - \frac{E}{R}$$

During the freewheeling interval the governing instaneous equation will be

$$E + L \frac{di_o}{dt} + R\, i_o = 0$$

As input supply is not connected to the output terminal

$$\text{So } \frac{di_o}{dt} + \frac{R}{L} i_o = -\frac{E}{L} \Rightarrow \frac{di_o}{-(\frac{E}{L} + \frac{R}{L} i_o)} = dt \Rightarrow \frac{L}{R} \ln[\frac{E}{L} + \frac{R}{L} i_o] + c = -t$$

At, $t = 0$ Let $i_o = I$ (say) So $\frac{L}{R} \ln[(\frac{E}{L} + \frac{R}{L} I)] + c = 0$

$$c = -\frac{L}{R} \ln \frac{E}{L} + \frac{R}{L} I$$

$$\text{So } \frac{L}{R} \ln(\frac{E}{L} + \frac{R}{L} i_o) - \ln(\frac{E}{L} + \frac{R}{L} I) = -t$$

$$\frac{L}{R} \ln \frac{\frac{E}{L} + \frac{R}{L} i_o}{\frac{E}{L} + \frac{R}{L} I} = - t \qquad \ln \frac{\frac{E}{L} + \frac{R}{L} i_o}{\frac{E}{L} + \frac{R}{L} I} = - \quad t/\tau$$

where $\tau = \frac{L}{R}$

$$\frac{E}{L} + \frac{R}{L} i_o = \left(\frac{E}{L} + \frac{R}{L} I\right) e^{-t/\tau}$$

$$\Rightarrow \frac{R}{L} i_o = - \frac{E}{L} + \frac{E}{L} e^{-t/\tau} + \frac{R}{L} I e^{-t/\tau}$$

$$\frac{R}{L} i_o = \frac{E}{L}\left[e^{-t/\tau} - 1\right] + \frac{R}{L} I e^{-t/\tau}$$

$$\Rightarrow i_o = \frac{E}{R}\left[e^{-t/\tau} - 1\right] + I e^{-t/\tau} \qquad ..(4.2)$$

During power interval instantaneous output current equation is

$$i_o = \frac{3\sqrt{6}\, E_{ph}}{Z} \sin(wt + \frac{\pi}{6} - \varphi) - \frac{E}{R} + K e^{-t/\tau}$$

Let at $t = t_o$; $i_o = I_o$

$$I_o = \frac{3\sqrt{6}\, E_{ph}}{Z} \sin(w\, t_o + \frac{\pi}{6} - \varphi) - \frac{E}{R} + K e^{-t_o/\tau}$$

$$K = I_o\, e^{t_o/\tau} + \frac{E}{R}\, e^{t_o/\tau} - \frac{3\sqrt{6}\, E_{ph}}{Z} \sin(w\, t_o + \frac{\pi}{6} - \varphi)\, e^{t_o/\tau}$$

$$\text{So } i_o = \frac{3\sqrt{6}\, E_{ph}}{Z} \sin(wt + \frac{\pi}{6} - \varphi) - \frac{E}{R} + I_o\, e^{-(t-t_o)/\tau}$$

$$+ \frac{E}{R}\, e^{-(t-t_o)/\tau} - \frac{\sqrt{6}\, E_{ph}}{Z} \sin(w\, t_o + \frac{\pi}{6} - \varphi)\, e^{-(t-t_o)/\tau}$$

$$i_o = \frac{3\sqrt{6}\, E_{ph}}{Z}\left[\sin(wt + \frac{\pi}{6} - \varphi) - \sin(w\, t_o + \frac{\pi}{6} - \varphi)\, e^{-(t-t_o)/\tau} \right]$$

$$+ \frac{E}{R}\left[e^{-(t-t_o)/\tau} \right] - 1 + I_o\, e^{-(t - t_o)/\tau} \qquad \ldots (4.3)$$

During the power interval i.e. $t_1 \leq t \leq t_2$

At the end of this interval i.e. at $t = t_2$; $i_o = I_2$;

According to equation 4.3

$$I_2 = \frac{3\sqrt{6}\, E_{ph}}{Z} \sin(wt_2 + \frac{\pi}{6} - \varphi) - \sin(wt_1 + \frac{\pi}{6} - \varphi) e^{-(t_2-t_1)/\tau}$$

$$- \frac{E}{R}\left[1 - e^{-(t_2 - t_1)/\tau}\right] + I_1\, e^{-(t_2-t_1)/\tau}$$

where I_1 is taken as the current at $t = t_1$

Let us suppose $A = \frac{3\sqrt{6}\, E_{ph}}{Z}\left[\sin(wt_2 + \frac{\pi}{6} - \varphi) \right.$

$$\left. - \sin(wt_1 + \frac{\pi}{6} - \varphi)\, e^{-(t_2-t_1)/\tau} \right] - \frac{E}{R}\left[1 - e^{-(t_2-t_1)/\tau}\right]$$

So $I_2 = A + I_1 e^{-(t_2-t_1)/\tau}$

During the freewheeling interval i.e. $t_2 \leq t \leq t_3$

At the end of this interval i.e. at $t = t_3$; $i_o = I_3$

According to equation 4.2

$$I_3 = \frac{E}{R}\left[e^{-(t_3-t_2)/\tau} - 1\right] + I_2 e^{-(t_3-t_2)/\tau}$$

$$= \frac{E}{R}\left[e^{-(t_3-t_2)/\tau} - 1\right] + I_1 e^{-(t_3-t_1)/\tau} + A e^{-(t_3-t_2)/\tau}$$

Let $\frac{E}{R}\left[e^{-(t_3-t_2)/\tau} - 1\right] + A e^{-(t_3-t_2)/\tau} = B$

So $I_3 = B + I_1 e^{-(t_3-t_1)/\tau}$

During the power interval i.e $t_3 \leq t \leq t_4$

at the end of this interval i.e. at $t = t_4$, $i = I_4$.

According to the equation 4.3

$$I_4 = \frac{\sqrt{6}\, E_{ph}}{Z}\left[\sin\left(wt_4 + \frac{\pi}{6} - \varphi\right) - \sin\left(wt_3 + \frac{\pi}{6} - \varphi\right) e^{-(t_4-t_3)/\tau}\right]$$

$$- \frac{E}{R}\left[1 - e^{-(t_4-t_3)/\tau}\right] + B e^{-(t_4-t_3)/\tau} + I_1 e^{-(t_4-t_1)/\tau}$$

Let us suppose first three terms in this equation is C

So $I_4 = C + I_1 e^{-(t_4-t_1)/\tau}$

During freewheeling interval i.e. $t_4 \leq t \leq t_5$

At $t = t_5$, $i_o = I_5$ So according equation 4.2

$$I_5 = \frac{E}{R}\left[e^{-(t_5-t_4)/\tau} - 1\right] + C\, e^{\frac{-(t_5-t_4)}{\tau}} + I_1 e^{-(t_5-t_1)/\tau}$$

Let us suppose first two terms is equal to D

So $I_5 = D + I_1 e^{-(t_5-t_1)/\tau}$

Similarway during power interval i.e. $t_5 \leq t \leq t_6$

At $t = t_6$, $i_o = I_6$, So according to the equation 4.3

$$I_6 = \frac{\sqrt{6}\, E_{ph}}{Z}\left[\sin\left(wt_6 + \frac{\pi}{6} - \varphi\right) - \sin\left(wt_5 + \frac{\pi}{6} - \varphi\right) e^{-(t_6-t_5)/\tau}\right]$$

$$- \frac{E}{R}\left[1 - e^{-(t_6-t_5)/\tau}\right] + D\, e^{-(t_6-t_5)/\tau} + I_1 e^{-(t_6-t_1)/\tau}$$

Let us suppose first three terms in this equation is equal to F

So $I_6 = F + I_1 e^{-(t_6-t_1)/\tau}$

During the freewheeling interval i.e. $t_6 \leq t \leq t_7$

At $t = t_7$; $i_o = I_7$ According to the equation 4.2

$$I_7 = \frac{E}{R}[\, e^{-(t_7-t_6)/\tau} - 1] + F\, e^{-(t_7-t_6)/\tau} + I_1\, e^{-(t_7-t_1)/\tau}$$

Let us suppose first two terms in this equation is equal to G

So $I_7 = G + I_1\, e^{-(t_7-t_1)/\tau}$

Similary, During $t_7 \leq t \leq t_8$

$$I_8 = \frac{\sqrt{6}\, E_{ph}}{Z} \sin(wt_8 + \frac{\pi}{6} - \varphi) - \sin(wt_7 + \frac{\pi}{6} - \varphi)\, e^{-(t_8-t_7)/\tau}$$

$$+ \frac{E}{R}[\, 1 - e^{-(t_8 - t_7)/\tau}] + G\, e^{\frac{-(t_8-t_7)}{\tau}} + I_1\, e^{-(t_8-t_7)/\tau}$$

Let the first three terms in this equation is H

So $I_8 = H + I_1\, e^{-(t_8-t_1)/\tau}$

During $t_8 \leq t \leq t_9$

$$I_9 = \frac{E}{R}\, [\, e^{-(t_9-t_8)/\tau} - 1] + H\, e^{-(t_9-t_8)/\tau} + I_1\, e^{-(t_9-t_1)/\tau}$$

Let first two term in this equation is I

So

$$I_9 = I + I_1 \, e^{-(t_9 - t_1)/\tau}$$

$$t_9 \leq t \leq t_{10}$$

$$I_{10} = \frac{\sqrt{6}\, E_{ph}}{Z} \left[\sin\left(wt_{10} + \frac{\pi}{6} - \varphi\right) - \sin\left(wt_9 + \frac{\pi}{6} - \varphi\right) e^{-(t_{10} - t_9)/\tau} \right]$$

$$+ I \cdot e^{-(t_{10} - t_9)/\tau} + I_1 \cdot e^{-(t_{10} - t_1)/\tau} + \frac{E}{R} \left[1 - e^{-(t_{10} - t_9)/\tau} \right]$$

Let first three terms in this equation is J

$$I_{10} = J + I_1 \, e^{-(t_{10} - t_1)/\tau}$$

$$t_{10} \leq t \leq t_{11}$$

$$I_{11} = \frac{E}{R} \left[e^{-(t_{11} - t_{10})/\tau} - 1 \right] + J \, e^{-(t_{11} - t_{10})/\tau} + I_1 \, e^{-(t_{11} - t_1)/\tau}$$

Let the first two terms in this equation is M

So $$I_{11} = M + I_1 \, e^{-(t_{11} - t_1)/\tau}$$

$$t_{11} \leq t \leq t_{12}$$

$$I_{12} = \frac{\sqrt{6}\, E_{ph}}{Z}\left[\sin(wt_{12} + \frac{\pi}{6} - \varphi) - \sin(wt_{11} + \frac{\pi}{6} - \varphi)\, e^{-(t_{12}-t_{11})/\tau} \right]$$

$$+ \frac{E}{R}\left[1 - e^{-(t_{12}-t_{11})/\tau}\right] + M\, e^{-(t_{12}-t_{11})/\tau} + I_1\, e^{-(t_{12}-t_1)/\tau}$$

Let us suppose first three terms in this equation is equal to N

Then

$$I_{12} = N + I_1\, e^{-(t_{12}-t_1)/\tau}$$

During the interval $t_{12} \leq t \leq t_{13}$

$$I_{13} = \frac{E}{R}\left[e^{-(t_{13}-t_{12})/\tau} - 1\right] + N\, e^{-(t_{13}-t_{12})/\tau} + I_1\, e^{-(t_{13}-t_1)/\tau}$$

Let us suppose

$$\frac{E}{R}\left[e^{-(t_{13}-t_{12})/\tau} - 1\right] + N\, e^{-(t_{13}-t_{12})/\tau} = P$$

and $e^{-(t_{13}-t_1)/\tau} = Q$

So

$$I_{13} = P + I_1 Q \qquad I_{13} - I_1 Q = P$$

As the current will repeat after 60° interval, so $I_{13} = I$

So $I_1 - I_1 Q = P$ $\qquad I_1 = \frac{P}{1-Q}$ ..(4.23)

As the initial current has been evaluated; so at any instant, the other initial currents like $I_2, I_3, \ldots, I_{12}$ can be evaluated.

Thus the nature of the steady-state current wave form is obtained.

After having the steady state output current waveform, the supply current waveform is being determined from the converter switching sequences as shown in Fig. 4.1(a). The input current waveform then is fourier analysed to get different harmonic contents. Thus the performance characteristics are determined by varying the speed of motor in a suitable step but keeping the modulating index constant. In that way, a set of performance characteristics for different modulating index m is obtained.

The performance characteristics and parameters are defined as follows :-

Speed Torque Characteristics : This characteristics shows the variation of motor speed with torque. So we may call that this characteristic is a measure of the speed regulation of the drive.

Displacement factor (DSPF) : Input current in any sort of converter scheme is not at all a pure sinusoid. So it consists of fundamental as well as harmonics. The phase angle of the fundamental current with respect to supply voltage is defined as fundamental or displacement angle. Cosine of this displacement angle is defined as displacement factor. Thus

$$DSPF = \cos\left(\tan^{-1}\left(\frac{a_1}{b_1}\right)\right)$$ where $a_1, a_2 \ldots, a_n$; $b_1, b_2 \ldots, b_n$ are the fourier coefficient of the input line current waveform.

Distortion factor (DSTF) : Distortion factor measures the amount of fundamental current present in the nonsinusoidal input current with respect to the r.m.s. value of input current.

$$DSTF = I_{IF} / I_{CIR}$$

where

I_{IF} → Input fundamental line current

I_{CIR} → Input r.m.s. line current.

Power Factor (PF) : It is a measure of the volt-ampere requirement of the drive system. It is defined as the ratio of the mean input power to the r.m.s. output voltamperes.

PF = Displacement factor x Distortion factor.

Harmonic Factor (HF) : The input current, being nonsinusoidal, constains currents of harmonic frequencies. Harmonic factor is defined as measure of harmonics contents in the input supply current and shows a measure of the distortion of the input current.

Thus

$$HF = \left[1 - \left(\frac{I_{IF}}{I_{CIR}}\right)^2\right]^{\frac{1}{2}}$$

Ripple Factor (RIF) : It is a measure of the ripple contents in the output current waveform.

Thus

$$RIF = \left[\left(\frac{I_{COR}}{I_{OCA}}\right)^2 - 1\right]^{\frac{1}{2}}$$

where

I_{COR} --> output r.m.s. current.

I_{OCA} --> output average current.

Peak Factor (PKF) : It is the ratio of the highest value of output ripple current to the lowest value of output ripple current in the output current waveform (instantaneous steady state waveform).

Thus

$$PKF = \frac{i_{OCP}}{i_{OCL}}$$

where

i_{OCP} → the highest value of ripple current in the instantaneous output curren in the steady state.

i_{OCL} → The lowest value of ripple current in the instantaneous output current waveform in the steady state.

Fig. 4.1(c) shows the flow chart to determine these performance characteristic and performance parameters.

In the next section, the performance characteristics for motoring operation of the drive machine are explained.

4.3 RESULTS AND DISCUSSIONS

The theoretical as well as experimental performance characteristics have been explained and shown in this section.

The speed-torque characteristics are shown in Fig. 4.2(a). The armature current is continuous because of very large number of pulses per half cycle in the equal pulse

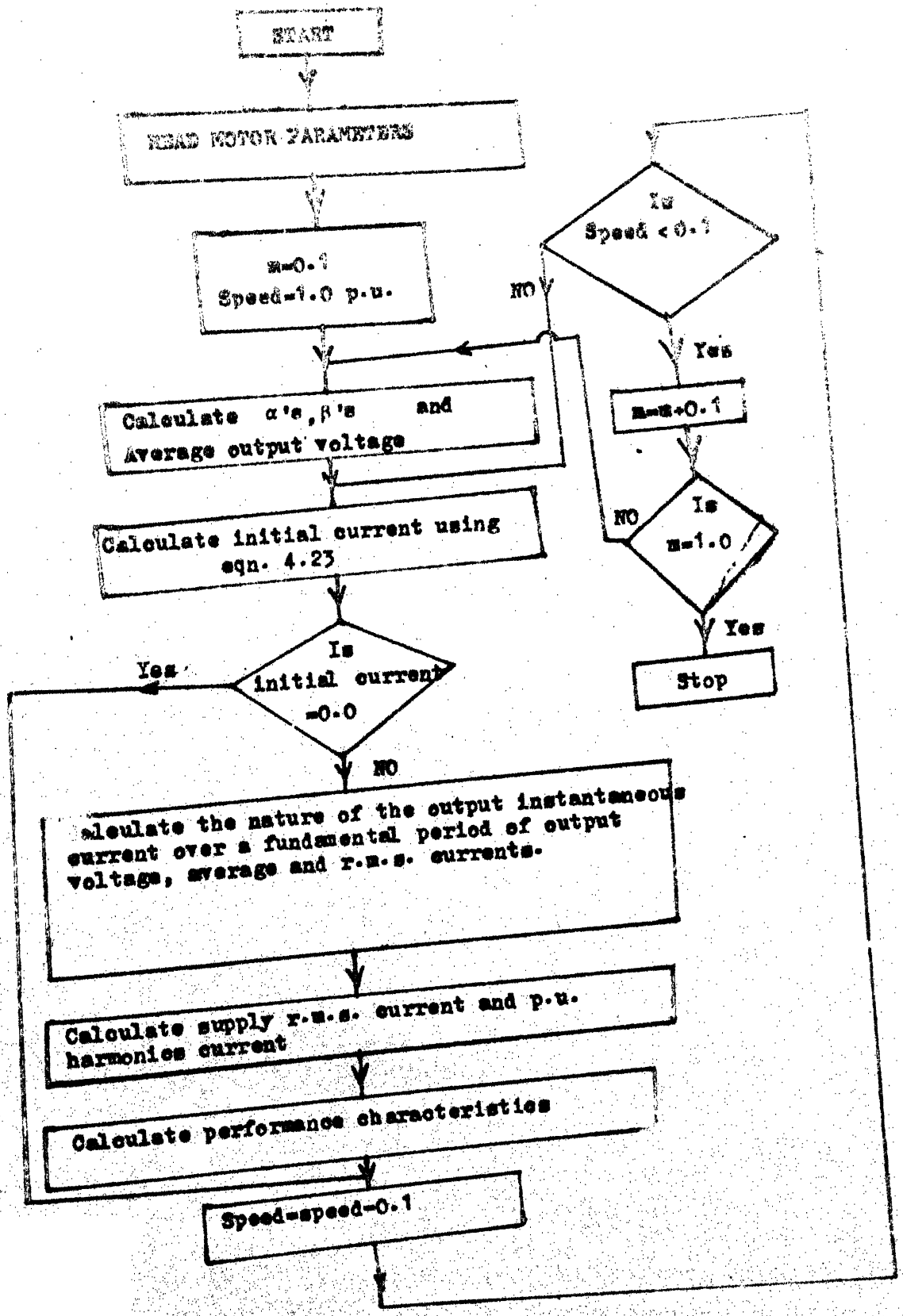

Fig.4.1(e) Flow Chart for the Calculation of Performance Characteristics for varying modulation index.

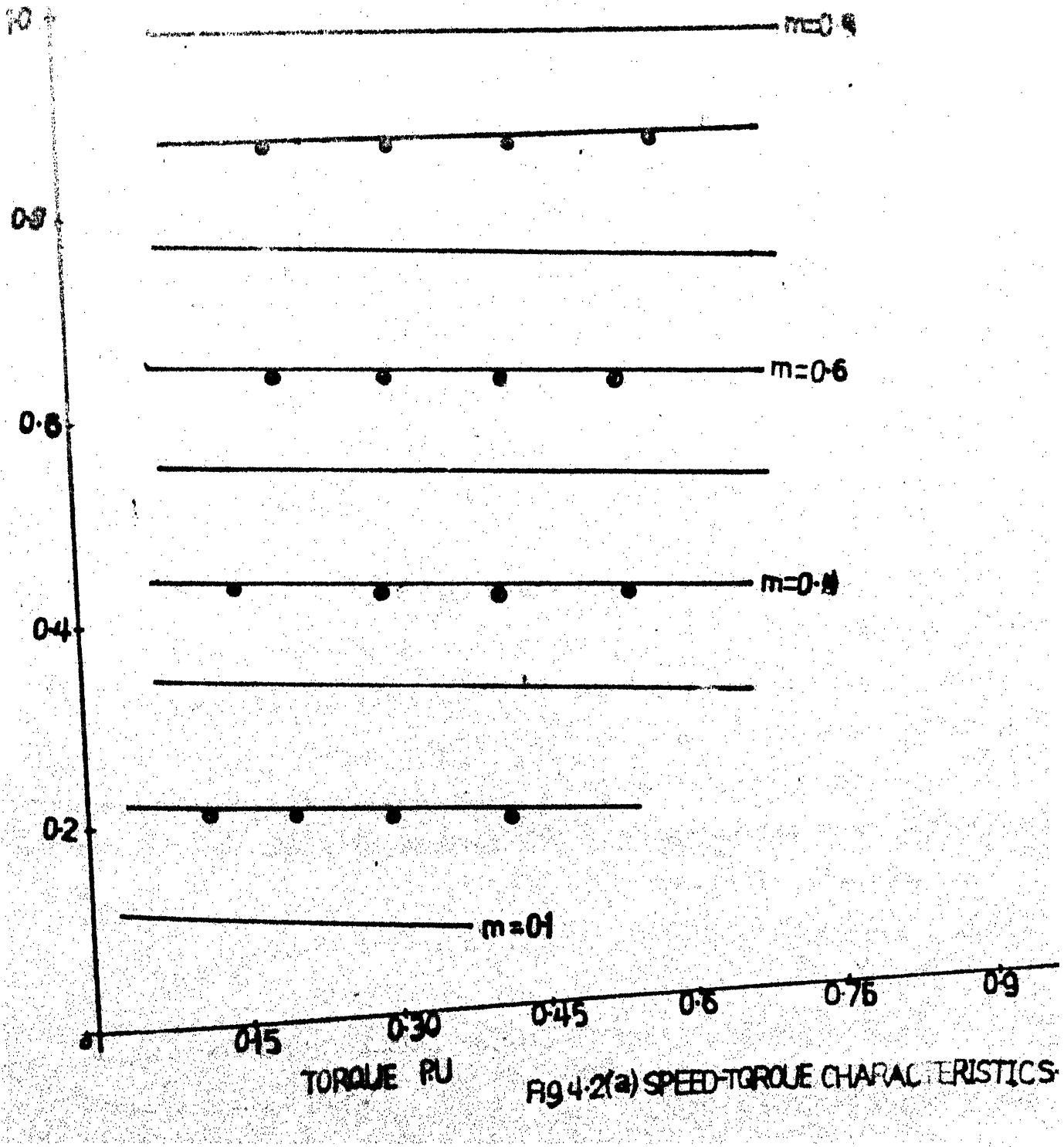

Fig 4.2(a) SPEED-TORQUE CHARACTERISTICS

width modulation technique adopted. The speed regulation is very good.

Fig. 4.2(b) - Fig. 4.2(e) shows the variation of displacement factor, harmonic factor, power factor, ripple factor, peak factor, distortortion factor w.r.t. speed for modulating index 0.1 - 0.9. The displacement factor is unity for all values of modulating index.

For a given modulating index, power factor decreases as the speed of the motor increases but power factor increases with an increase in modulating index for a particular speed of the motor.

The distortion factor for a given modulating index decreases as the speed of the motor increases but distortion factor increases with an increase in modulating index for a particular speed of the motor. But it has been found that the variation of distortion factor w.r.t. speed for a given modulating index is nearly same

For a given modulating index, the harmonic factor increases as the speed of the motor increases but harmonic factor decreases with an increase in modulating index for a particular speed of the motor. But it has been found that for higher modulating index, harmonic factor is less for a particular speed of the motor.

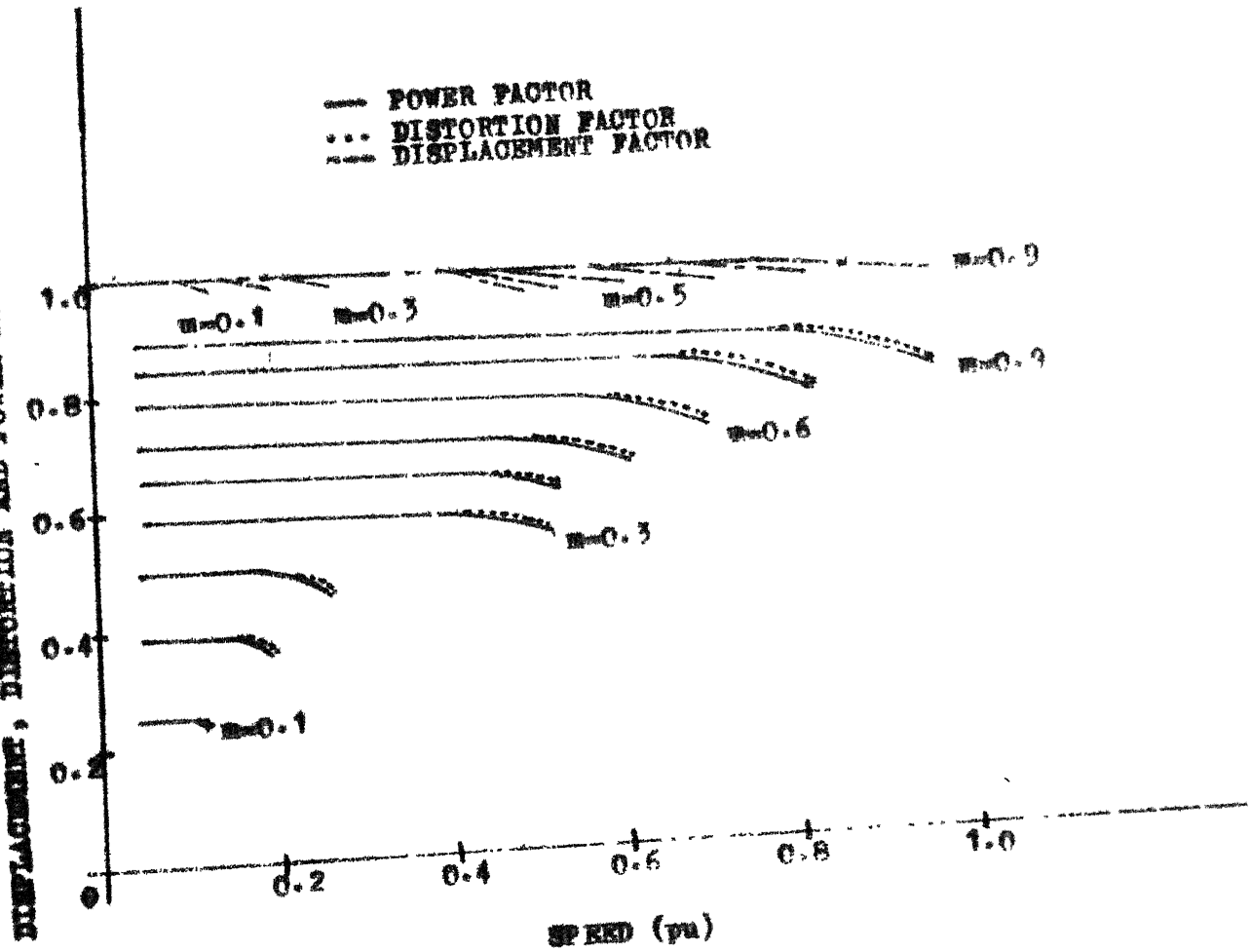

Fig. 4.2(b) SPEED Vs. DISPLACEMENT, DISTORTION AND POWER FACTORS FOR DIFFERENT VALUES OF MODULATION INDEX.

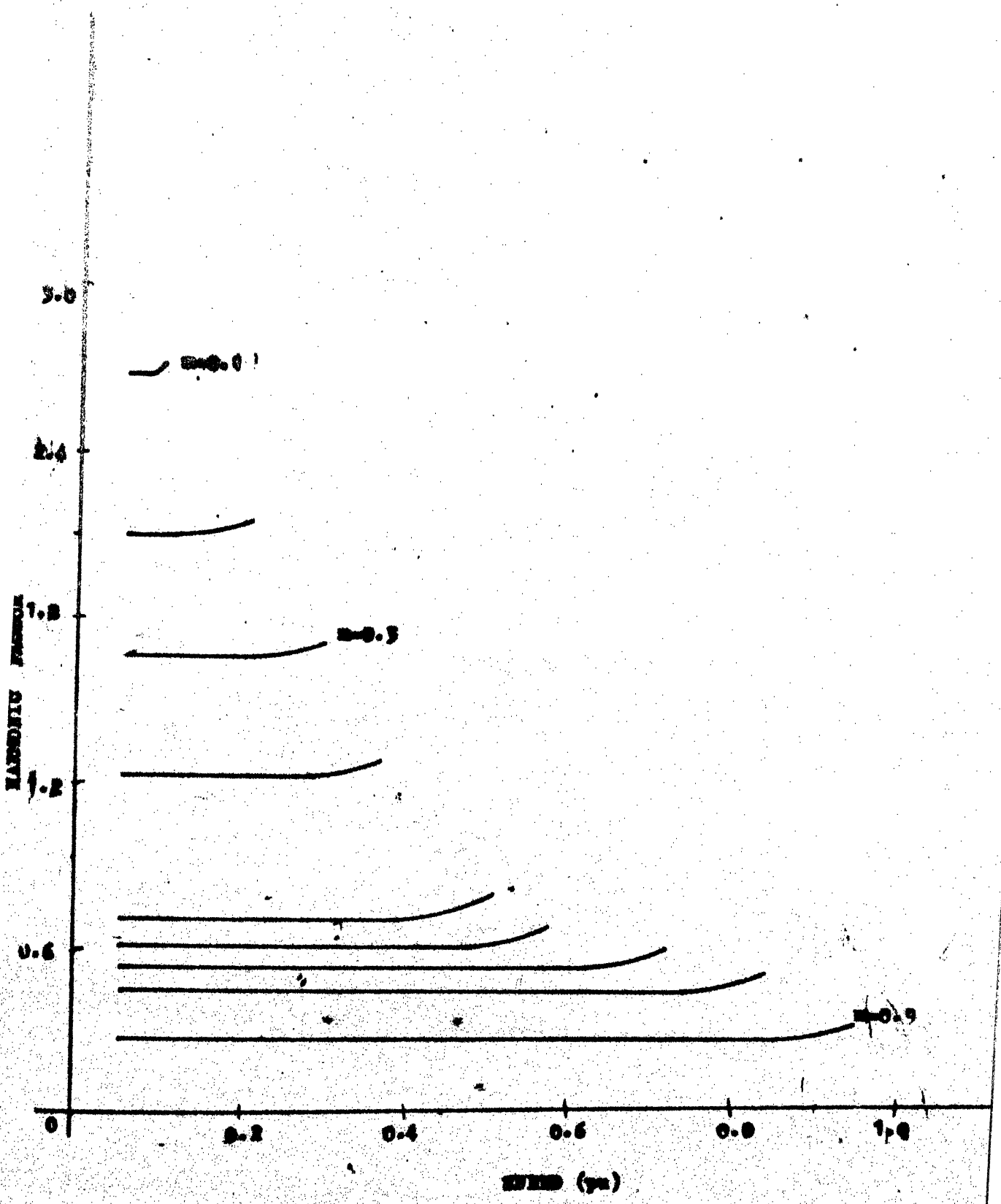

Fig. 4.2(a) SPEED Vs. RANDOMIZE FACTOR FOR DIFFERENT VALUES OF MODULATION INDEX

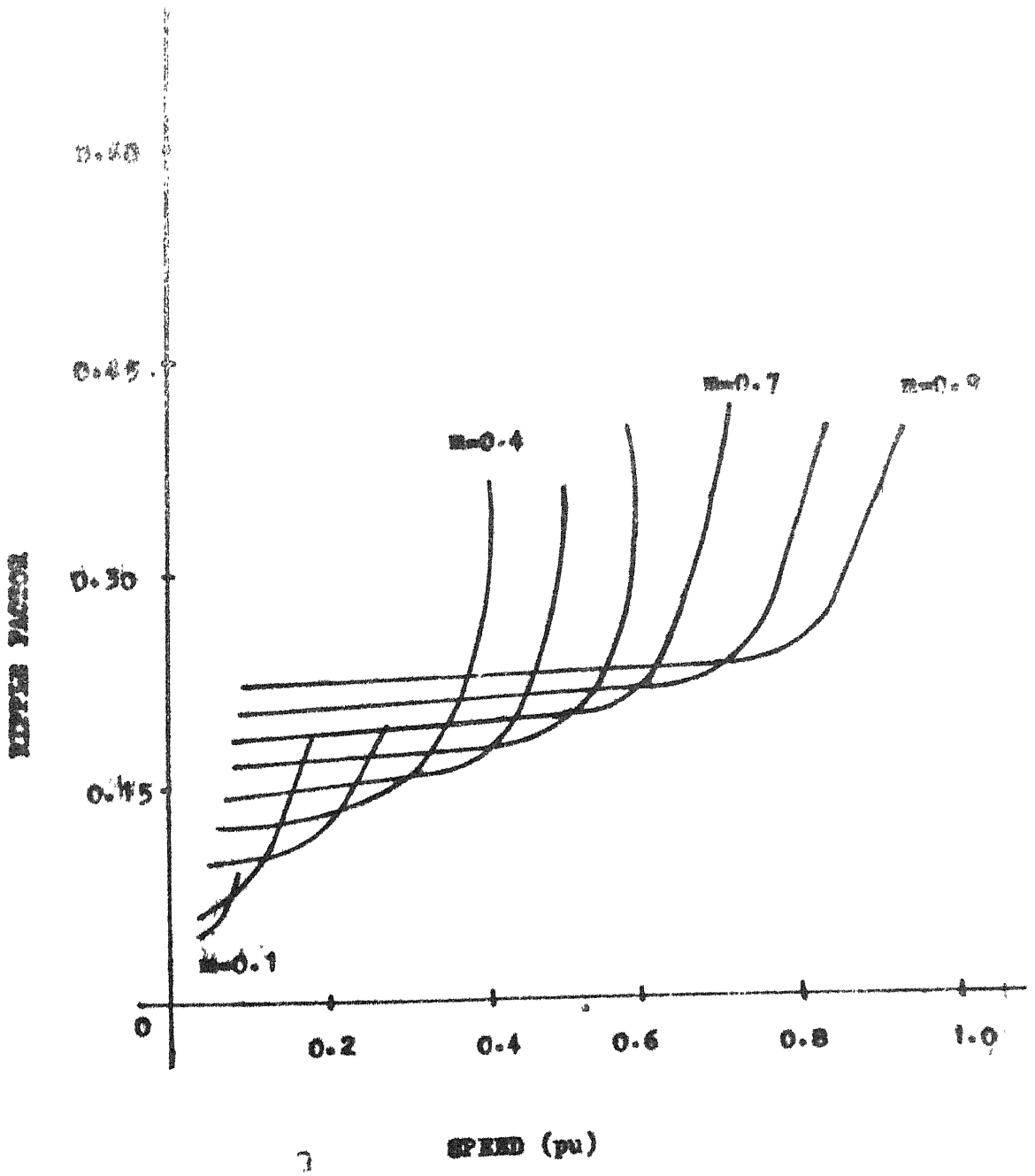

Fig. 4.8(d) SPEED Vs. RIPPLE FACTOR FOR DIFFERENT VALUES OF MODULATION INDEX

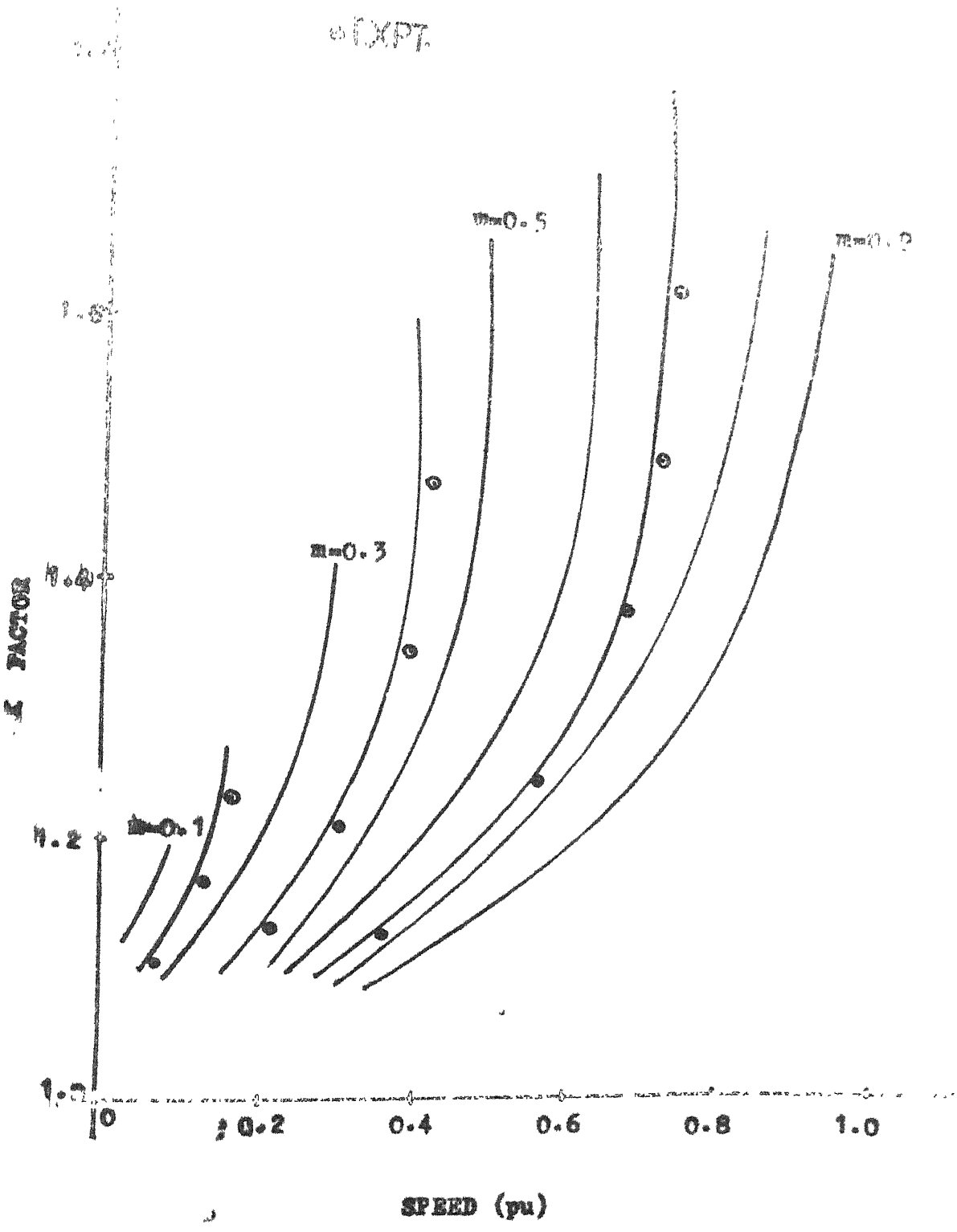

Fig. 4.2(e) SPEED Vs. PEAK FACTOR FOR DIFFERENT VALUES OF MODULATION INDEX

For a given modulating index, peak factor increases with the increase in speed of the motor but for a particular speed, peak factor decreases with the increase of the modulating index. In lower range of the speed of the motor, peak factor decrement with the increment of the modulating index is somewhat less but in the upper speed ranges of motor, peak factor decrement with the increment of the modulating index is somewhat abrupt or large.

For a given modulating index; ripple factor increase with the increase in speed of the motor but ripple factor decreases as the modulating index increases. In the lower range of speed of the motor, decrement of ripple factor with the increment of the modulating index is somewhat less but in the upper speed range of the motor, this variation is somewhat abrupt.

4.4 PERFORMANCE CHARACTERISTICS UNDER CONSTANT TORQUE OPERATION

Separately excited dc motors provide constant torque characteristics if the load current is maintained constant and armature voltage is controlled. These performance characteristics are being studied under constant torque operation by digital simulation. In this study, the converter circuit is

assumed to operate with equal pulse-width modulation (EPWM) control technique.

Fig. 4.3(a) shows the flow chart to determine these performance characteristics under constant torque operation of the separately excited motor.

4.5 RESULTS AND DISCUSSIONS UNDER CONSTANT TORQUE OPERATION

In this section, the performance parameters under constant torque operation of the motor in the motoring mode have been discussed. In what follows, the performance parameters are presented for 100%, 75%, 50% of the rated torque of the motor. Fig. 4.3(b) shows the variation of the performance parameters like displacement factor, distortion factor, power factor, harmonic factor, peak factor, ripple factor w.r.t speed variation of the motor for 100%, 75%, 50% of the rated torque of the motor under constant torque operation of motor in the motoring mode.

For a given torque, displacement factor is unity at any speed of the motor and it is also unity at any torque operation of the motor.

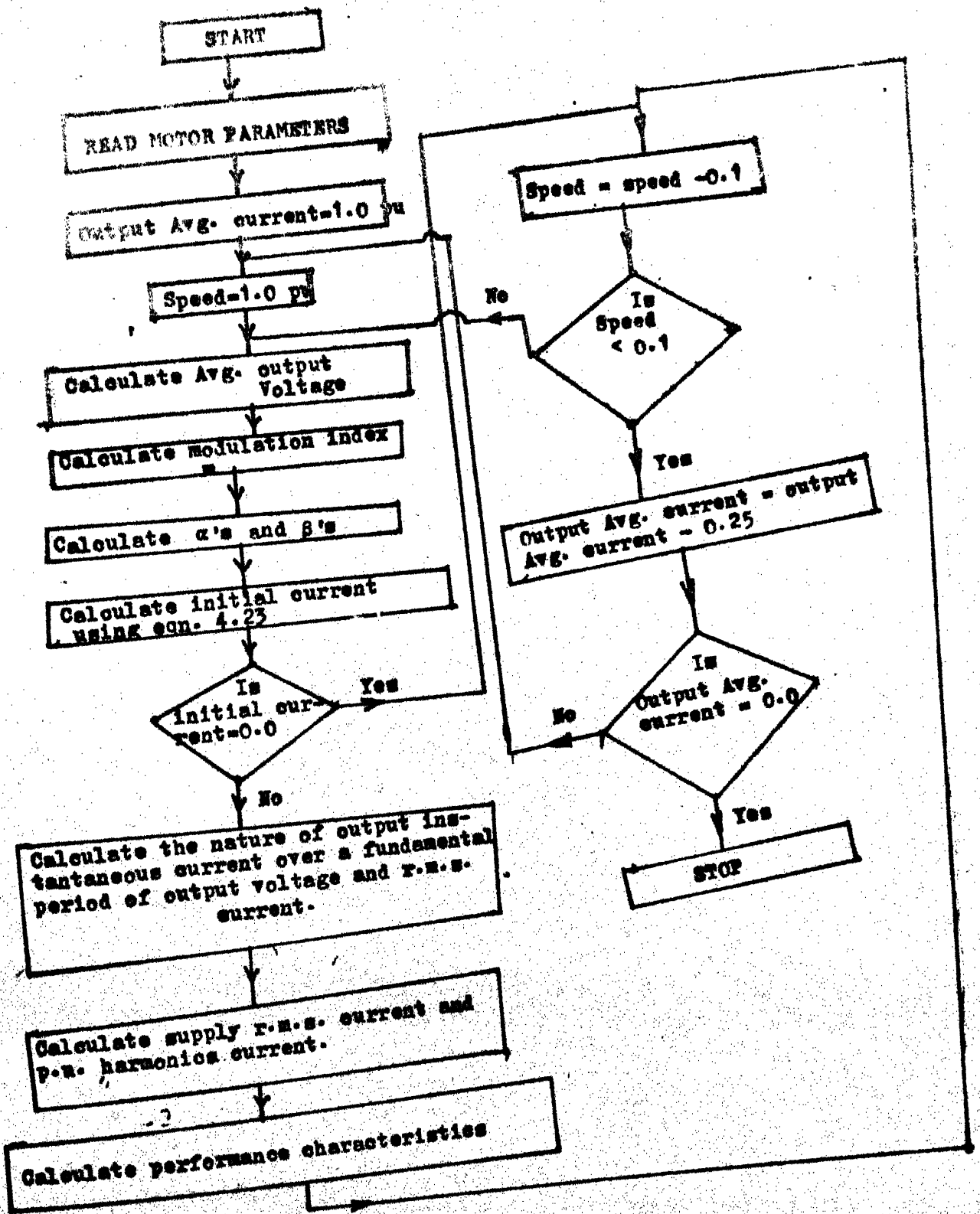

Fig. 4.3(a) Flow Chart for the Calculation of performance characteristics at constant torque.

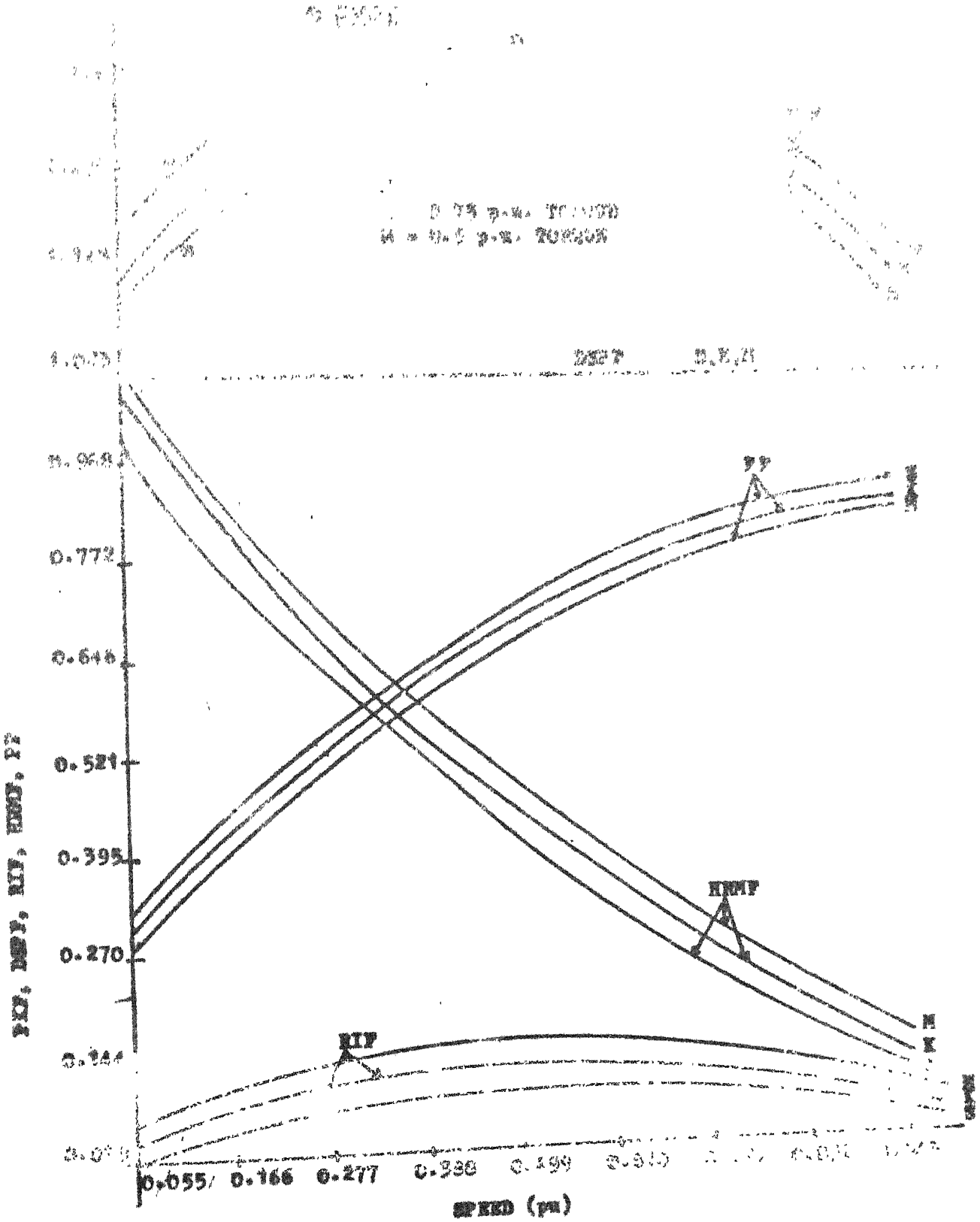

Fig. 4.3(b. SPEED Vs. POWER FACTOR, HARMONIC FACTOR, RIPPLE FACTOR, DISPLACEMENT FACTOR, PEAK FACTOR FOR DIFFERENT VALUES OF CONSTANT TORQUE WITHOUT INPUT FILTER

For any given torque, power factor increases as the speed of the motor increases but upto 60% rated speed of the motor, increment is much more than that of rest part of the speed attained by the motor. For a particular speed of the motor, power factor detoriates as the constant torque decreases.

At any constant torque, the harmonic factor decreases as the speed increases but for a particular speed, harmonic factor increases as the constant torque decreases.

For any given torque, ripple factor increases upto 50% rated speed attained by the motor but then decreases, as the speed next increase from 60% to 100% of the rated speed. But for a particular speed, ripple factor increases as the constant torque decreases.

For a given constant torque, peak factor increases as the speed increases but it is limited upto 50% rated speed attained by the motor and in the later part, as the speed further increases, peak factor decreases. But for a particular speed, peak factor increases as the constant torque decreases.

4.6 INPUT SUPPLY HARMONICS SPECTRA

Fig. 4.3(c) shows the amplitude variations of dominant input supply current harmonics with speed variation as well as the constant torque variation of motor. Because of EPWM with eighteen number of pulses per half cycle, the harmonic spectrum has shifted from lower order to higher order frequency components. Triplen harmonics are absent because of three phase configuration. The dominant harmonics are seventeenth and nineteenth. Since, there is halfwave symmetry in the input supply current, even harmonics are absent. At low speed 17th and 19th harmonics are quite significant but as the speed increases, they decrese gradually. Other predominant harmonics in the order of their magnitude in the low frequency region are 5th, 7th, 11th, 13th. They are of low amplitude and their variations with speed and torque are quite insignificant. For a particular speed, the harmonics decreases slightly with an increase in load torque. The other higher order harmonics like 23rd, 25th are present but they are of low amplitude over the entire range of speed.

4.7 PERFORMANCE CHARACTERISTICS WITH INPUT FILTER

In the section 4.6, it has been found that only 17th and 19th harmonics in the supply current are more pro-

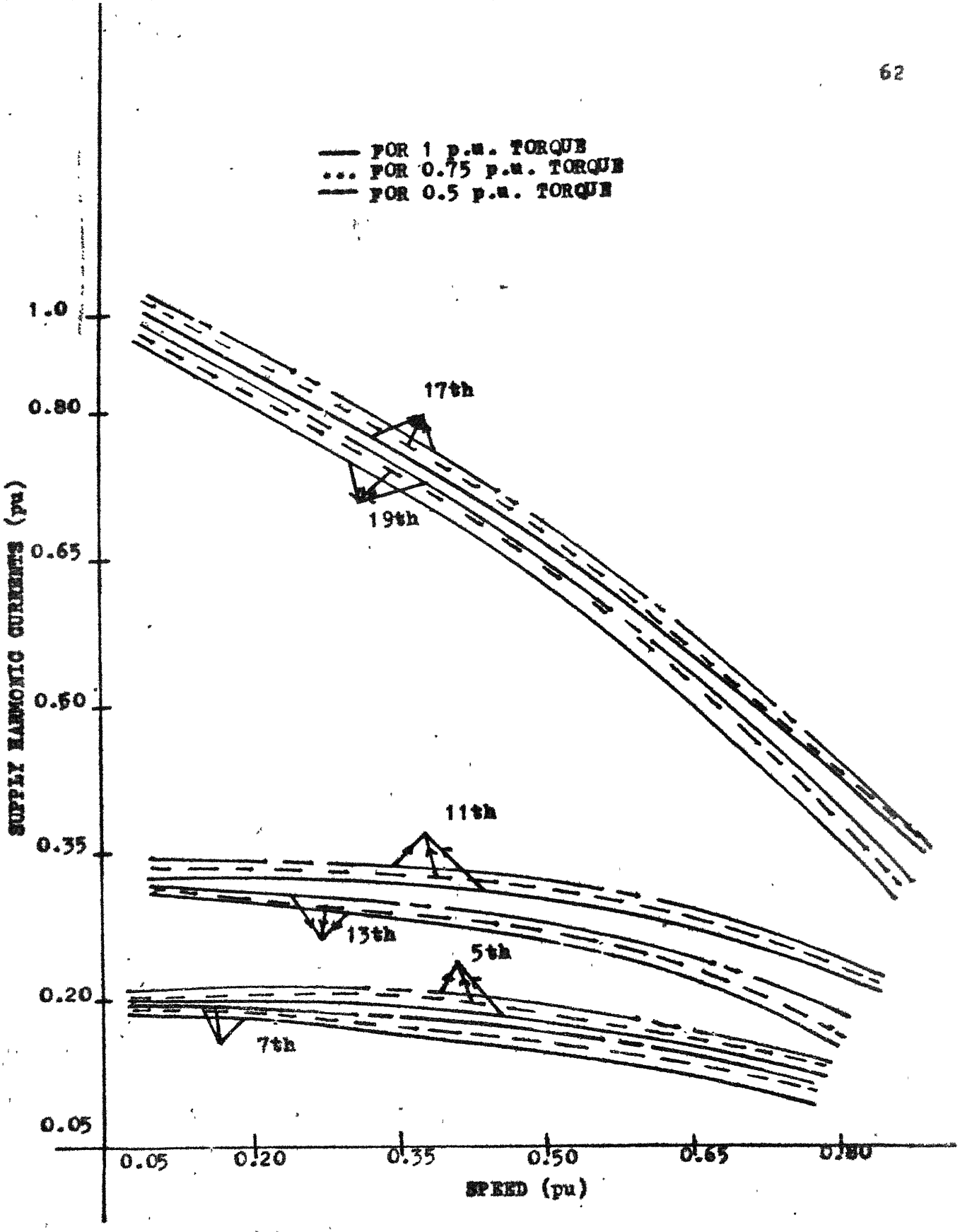

Fig. 4.3(e) SPEED vs. SUPPLY HARMONIC CURRENTS AT DIFFERENT VALUES OF CONSTANT TORQUE

minent in the low speed region but the other harmonics in the supply current are quite insignificant in the entire speed region. In order to improve the performance characteristics, suppression of these 17th and 19th harmonics in the supply current is desired. An input filter can eliminate most of the harmonics currents from the supply line, thereby making the line current essentially sinusoidal. Thus a low pass filter of resonance pulsation Wr slightly less than the 17th harmonic frequency has been designed and put in the input side of the converter. This section has already received some attention as exemplified by refs. [9] and [16] .

The input filter design and the performance analysis of converter-motor system with input filter presented in this section have been obtained with the assumptions that :

i) The input voltage of three phase ac-dc converter is purely sinusoidal.

ii) The switching elements in this converter are ideal.

iii) The input filter components are ideal.

iv) The load current is ripple free.

Let Wr be the resonance pulsation of the input filter. W_r is taken as 800 Hz.

$$W_r = \frac{1}{\sqrt{LC}} \qquad C = 50\mu F$$

$$L = \frac{1}{W_r^2 C} = \frac{1}{(2\pi x800)^2 x50x10^{-6}} H = 13mH$$

So filter componets are C = 50μF and L = 13 mH

Fig. 4.4 shows the improved performance characteristics like displacement factor, power factor, harmonic factor with input filter taken into account. These performance characteristics have been plotted against the p.u. speed of motor under constant torque operation of the motor. With input filter, the peak factor is unity because of ripple free load current and ripple factor is zero. Rating of L and C are given in Appendix B.

4.8 EXPERIMENTAL OSCILLOGRAMS

Experimental oscillograms are illustrated in Fig. 4.5. Different waveforms like output voltage, output current, input voltage, input current, transistor base-collector

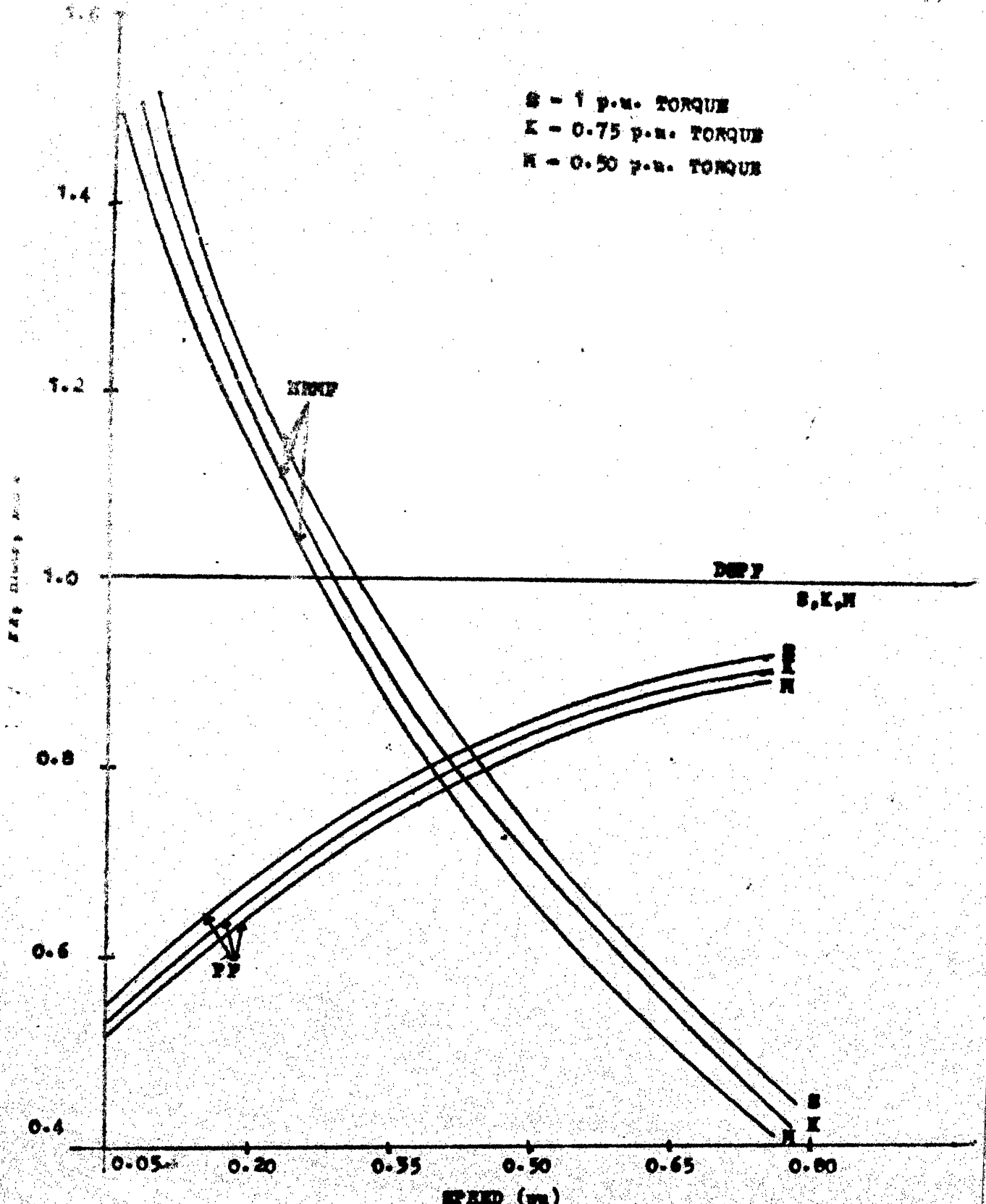

Fig. 4.4 SPEED Vs. POWER FACTOR, DISPLACEMENT FACTOR, HARMONIC FACTOR FOR DIFFERENT VALUES OF CONSTANT TORQUE WITH INPUT FILTER.

voltage and emitter collector voltage are shown at 0.6 modulating index with the motor running at light as well as heavy load. These oscillograms illustrate the basic principles of operation of the converter and verify the working of the circuit.

Scale - V_A = 10V/Div, V_o = 10V/div, i_A = 1A/div , i_o = 1A/div

Time = 4 msec/div.

Fig. 4.5(a) WITHOUT FILTER

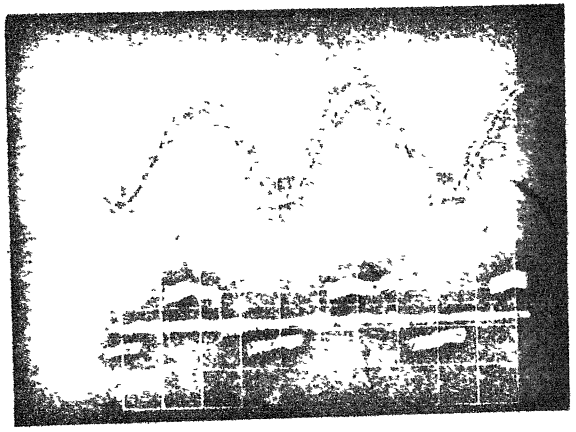

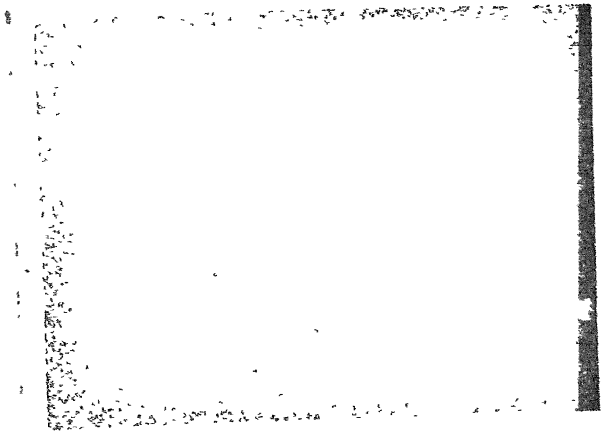

Scale - V_A = 100V/div, V_o = 100V/div, i_A = 8A/div, i_o = 8A/div

Time = 4 msec/div

Fig. 4.5(b) WITHOUT FILTER

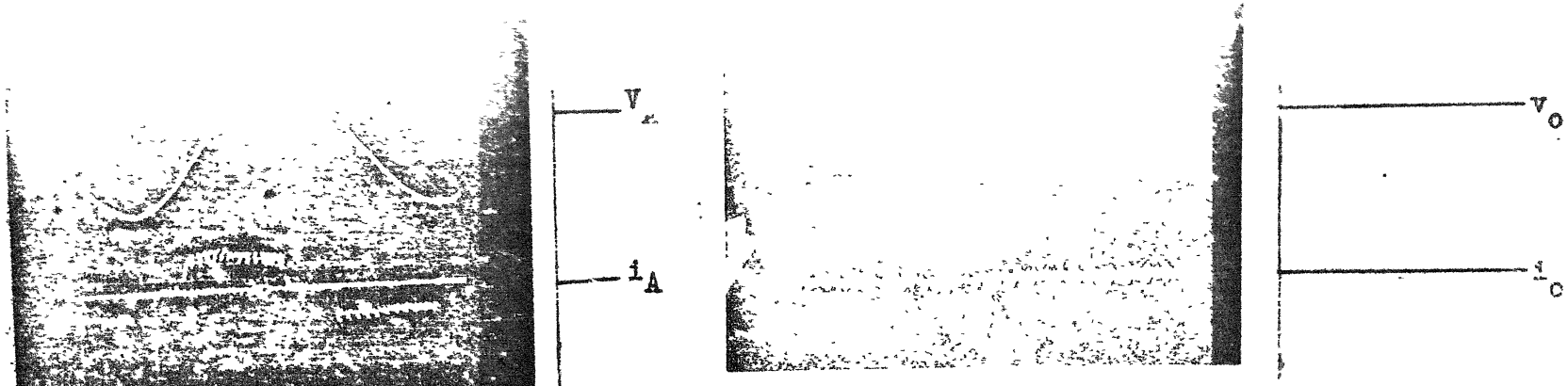

V_A = 10V/Div, V_o = 10V/div, i_A = 1A/div, i_o = 1A/div

Time = 8 msec/div

Fig. 4.5(c) WITH FILTER

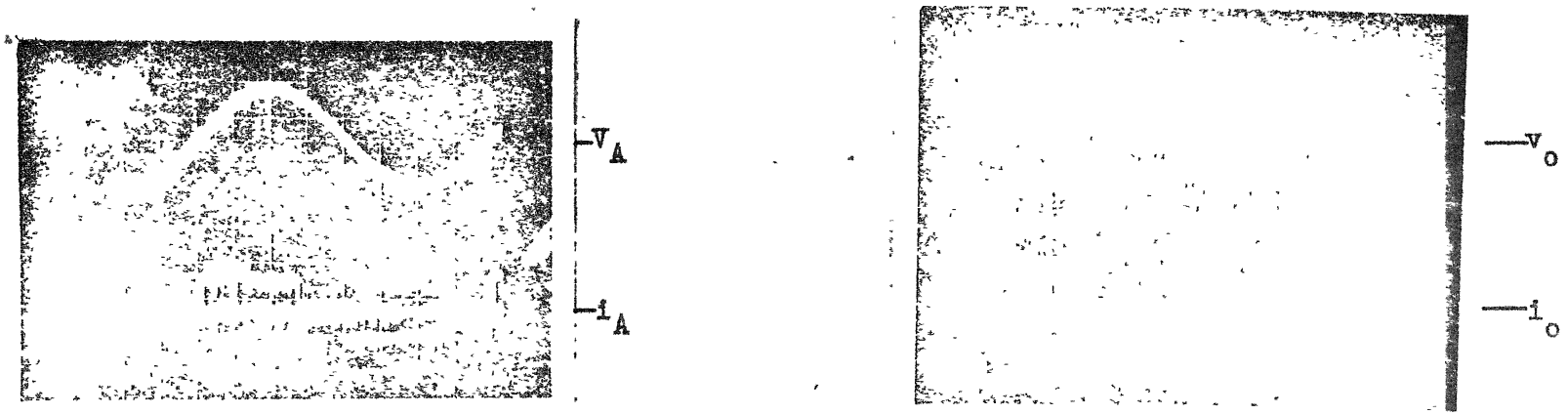

Scale - V_A = 100V/div, V_o = 100V/div, i_A = 8A/div, i_o = 8A/div

Time [illegible] msec/div, 4 msec/div.

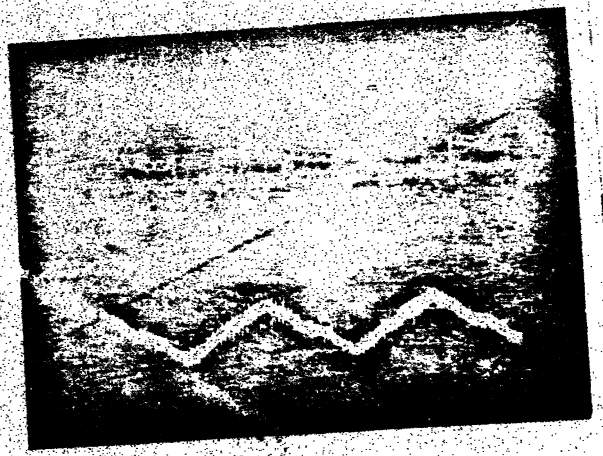

Scale - V_{CB} = 0.4V/div

V_{CE} = 0.5V/div

Time = 4 msec/div

Fig. 4.5(e)

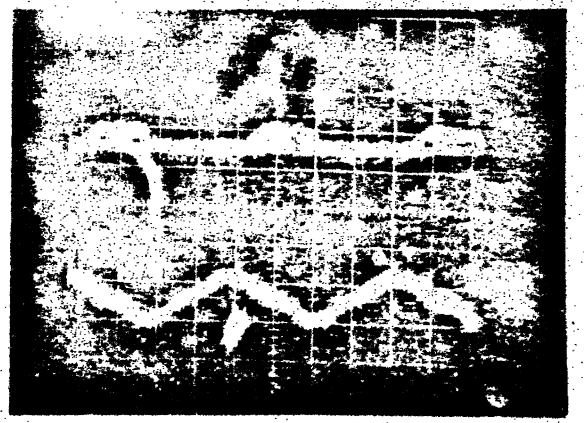

Scale V_{CB} = 0.7V/div

V_{CE} = 0.5V/div

Time = 4msec/div

Fig. 4.5(f)

CHAPTER 5

CLOSED-LOOP VOLTAGE CONTROL OF THREE-PHASE AC-DC CONVERTER

5.1 INTRODUCTION

The converters are widely used in many applications where the output power control is required. The open-loop operation of converter may not be satisfactory in many applications. However, if the application demands variable output voltage, the firing angle is to be changed in order to achieve the desired output voltage. This can be achieved in a closed loop control system. A closed-loop control system generally has the advantage of greater accuracy, improved dynamic response and reduced effects of disturbances because one of the primary objectives of using feedback in the control system is to reduce the sensitivity of the system to parameter variations. The parameters of the system may vary with age, with changing environment (e.g., ambient temperature), etc. Conceptually, sensitivity is a measured of the effectiveness of feedback in reducing the influence of these variations on system performance. In the closed-loop control, the protection of solid state devices must be ensured.

5.2 STATIC POWER SUPPLY

The converters are widely used for precision control of the output power in many industrial applications. One of the primary methods of getting a variable converter output voltage is to incorporate closed-loop for the output current of the converter. This scheme is shown in Fig. 5.1. Where, I_R is used to set the reference output current of the converter. The signal I_A representing the actual output current of the converter is passed through a low pass filter, and is compared with the reference current. The error signal ε_I is fed to the current controller which is generally a PI controller because it provides zero steady state error for the output current. The output current is sensed by a current transducer.

5.3 CLOSED-LOOP CONTROL OF THE OUTPUT CURRENT

The output voltage is controlled through the output current control loop. The realisation of the closed-loop control system is discussed in the following sections.

5.3.1 Current Sensor

The output current control loop requires a signal which should be proportional to the output current of the

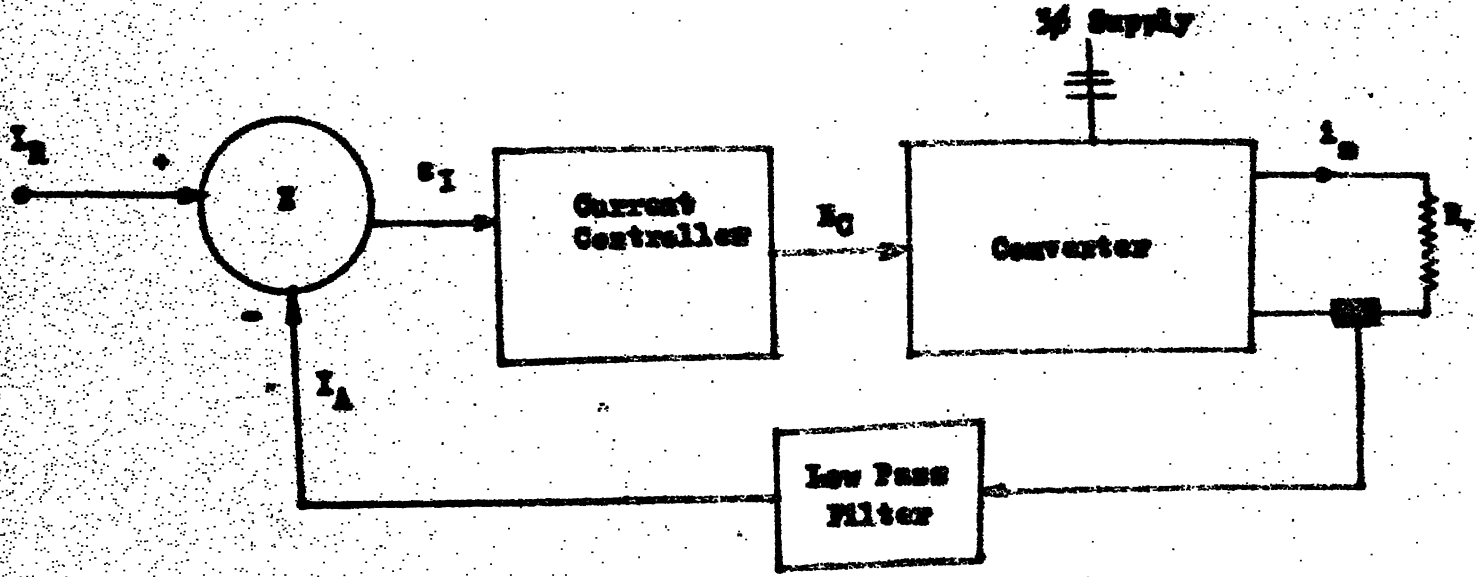

Fig. 5.1 BLOCK DIAGRAM OF CLOSED-LOOP CONTROL SYSTEM

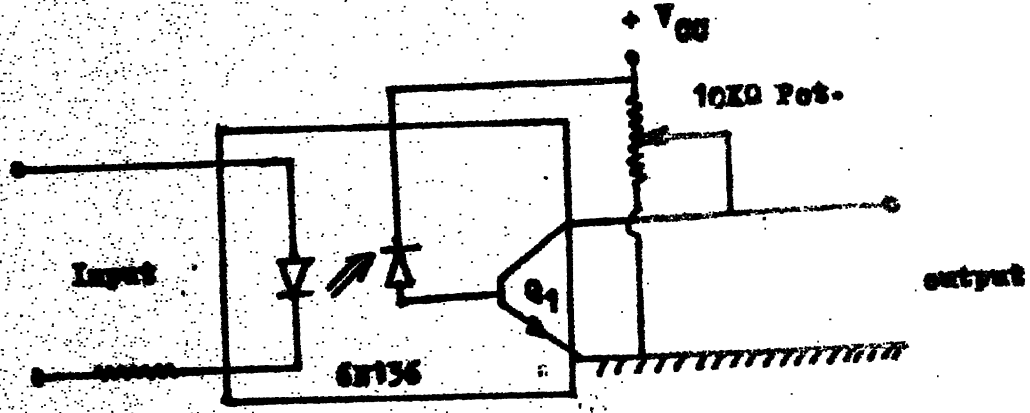

Fig. 5.2 CURRENT SENSOR

converter. The current is sensed by sensing a voltage signal across a small resistor connected in series with the load. The signal is fed to an optoisolator stage as shown in Fig. 5.2. This current signal drives the base of the transistor Q_1. Q_1 is biased to operate in the switching mode using 10 K-ohms potentiometer. Thus, a current signal which is completely isolated and proportional to the load current from the power circuit is obtained.

5.3.2 Current Controller

There are two common types of current controllers used in practice :

(i) Proportional (P) controller.

(ii) Proportional plus integral (PI) controller.

The proportional controller gives significant amount of steady state error because the output signal proportional to the actuating signal whereas PI controller gives zero steady state error because the output signal here is proportional to the actuating signal plus integral to the actuating signal. Thus, a PI controller has been chosen for the output current control loop.

5.3.3 Firing Circuit

The analog firing circuit as discussed in Chapter 3 is used. The relationship between the average output voltage of the converter and the modulation index m is found to be linear. The average output voltage E_o of the converter is given by

$$E_o = \frac{3\sqrt{6}}{\pi} E_{ph} \, m$$

where E_{ph} is the rms value of supply voltage per phase.

$$m = \frac{V_{mm}}{V_{cm}}$$

where V_{mm} is the amplitude of the modulating signal and V_{cm} is the amplitude of the carrier signal.

As the amplitude of the carrier signal V_{cm} = 5 Volts,

$$E_o = \frac{3\sqrt{6}\, E_{ph}}{\pi} \cdot \frac{V_{mm}}{5}$$

Let $K = \frac{3\sqrt{6}\, E_{ph}}{5\pi}$, $E_c = V_{mm}$

$$E_o = K E_c$$

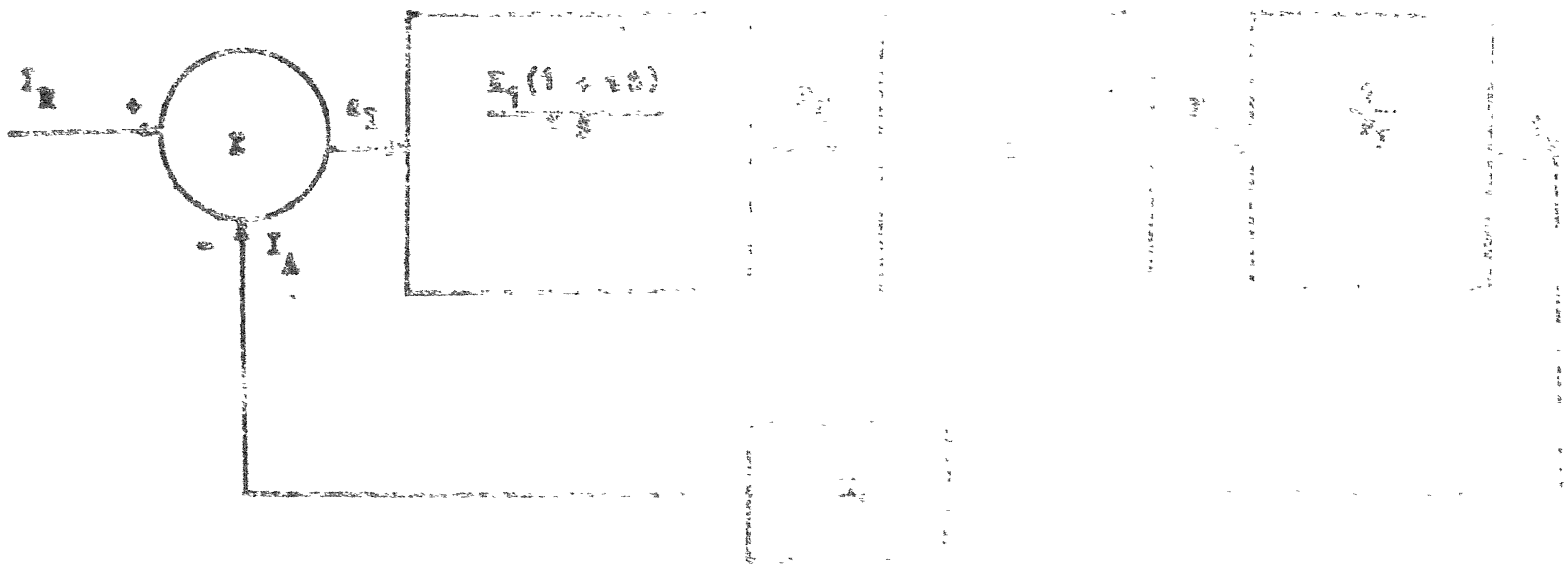

Fig. 5-3 TRANSFER FUNCTION OF EACH BLOCK

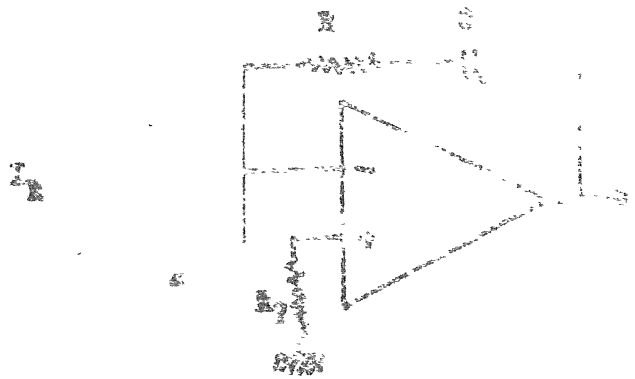

Fig. 5-4 [illegible]

5.4 DESIGN OF CURRENT CONTROLLER

The block diagram of the current control loop with the PI controller is shown in Fig. 5.3. The PI current controller logic circuit is shown in Fig. 5.4.

Here $\tau = RC$, $K_1 = \frac{R}{R_2}$

The transfer function of the PI current controller is

$$\frac{K_1(1 + S\tau)}{S\tau}$$

The loop gain function as shown in Fig. 5.3 is

$$G H_1(S) = \frac{K K_1(1 + \tau S) H_1}{R_L \tau S}$$

Choosing τ = 5 msec, for different values of K_1, it has been found that the current loop response will be fast for K = 2

As C is chosen to be 0.5 μF, $R = \frac{5 \times 10^{-3}}{0.5 \times 10^{-6}} = 10$ K-ohms

As $K_1 = 2$, $R_2 = \frac{10}{2}$ K-ohm = 5 K-ohms.

For the maximum converter output current of AOA, R_1 is chosen to be 18 K-ohms considering the saturation voltage of the operational amplifier configuring the PI controller.

5.5 REALISATION OF THE CLOSED-LOOP CONTROL SCHEME

Fig. 5.5 shows the logic circuit with which the closed-loop control can be achieved. In the closed-loop control system, the voltage from potentiometer P represents the reference current (I_R of Fig. 5.5). The signal I_A represents a voltage proportional to the load current of the converter. A low pass active filter Q_2 eliminates the high frequency ripples in the load current i_a. A PI controller Q_3 provide the gain and desired response. The zener diode D_Z is used to limite the output of Q_4 to a predetermined maximum voltage. To limit the current through the zener diode D_Z, a resistance having 1 K-ohm value is connected in series with the zener diode. The output voltage of Q_4 is the control voltage E_C of the converter. By changing this control voltage E_C, the desired converter output voltage can be obtained.

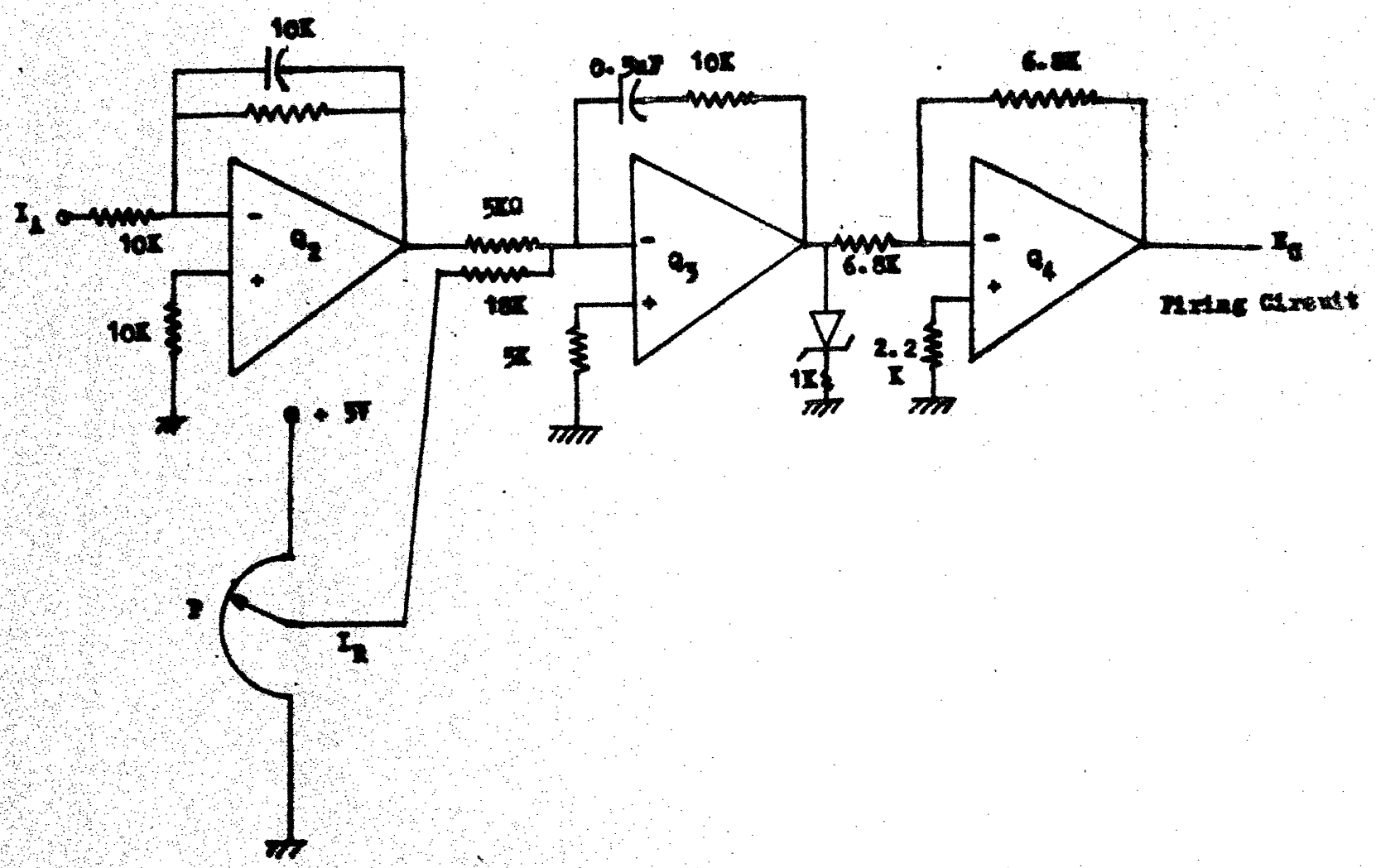

Fig. 5.5 LOGIC CIRCUIT FOR CLOSED-LOOP CONTROL SYSTEM.

CHAPTER 6

CONCLUSION

6.1 CONCLUSION

A simple three-phase ac-dc power transistor converter is investigated in this thesis. The power transistor converter if properly designed and protected has an edge over the thyristor converter since it require no commutation circuitry. The EPWM with eighteen pulses per half-cycle of the supply voltage provides a smooth variation of the output voltage from zero percent to cent percent of the maximum output voltage. The experimental study has revealed that the converter has provided satisfactory operation with R, R-L, dc motor loads. LC filter has been designed to reduce or eliminate the predominant harmonic in the supply system. The transistor converter improves input and output performances, and has all the advantages associated with a thyristor converter [14] reported earlier. Since a power transistor is employed as the basic building block in the converter, this has made it possible to extend the frequency of switching resulting in the output current which is almost ripple free. Also, the input current harmonic spectrum has shifted from lower order to the higher order (17th & 19th) because of the high frequency

of operation. The performance of the power transistor converter with regard to the output current is almost similar to that of an M-G set. The converter is quite suitable not only for the speed control of a dc motor but also for the variable dc power source. The power rating of the converter however is limited depending upon the voltage and current ratings of the power transistors commercially available at the present time.

6.2 FURTHER SCOPE OF WORK

The steady state and transient performance of an ac-dc power transistor converter fed dc series motor can be investigated. Both open-loop and closed loop studies may be carried out.

REFERENCES

1. V.R. Stefanovic, 'Power factor improvement with modified phase controlled converter,' IEEE Trans. Ind. Appll, vol. - IA - 15, pp 193, 1979.

2. T. Ohmishi and H. Okitsn, 'Bias voltage controlled three phase converter with high power factor', IEEE Trans. Ind. Appl., vol. IA-16, pp. 700, 1980.

3. W. Mcmurray, 'A study of asymmetrical gating for phase controlled converters', IEEE Trans. Ind. Appl., vol.IA-8, pp. 289, 1972.

4. T. Kataoks, K. Mizumechi and S. Miyairi, 'A pulse width controlled AC to DC converter to improve power factor and waveforms of AC line current', IEEE Conference Record, ISPCC-77, New York, 1977.

5. P.C. Sen and S.R. Doradla, 'Evaluation of control schemes for thyristor controlled DC motors', IEEE Trans. IECI, vol. IECI-25, No.3, 1978.

6. R.K. Abrol, 'Investigations on a improved forced commutation scheme and its application in static control of DC and AC drives', Ph.D. Thesis, IISc Bangalore, 1979.

7. P.C. Sen, 'Thyristors DC drives', A Wiley interscience publication, John Wiley and Sons, New York.

8. B.R. Pelly and S. Clemente, 'Understanding Power MOSFETS switching performance', International Rectifier Corporation, EI Segundo, California, A. Isidon, University of Rome, Italy

9. P.D. Ziggas, Young-Goo Kang and V.R. Stefanovic, 'PWM control techniques for rectifier filter minimization', Dept. of Electrical Engineering, Concordia University, Montreal, Quebec, Canada.

10. Marlen Varnovistsky, 'Development and comparative analysis of a pulse width modulation strategy', IEEE Trans. IE., vol. IE-31, No. 3, 1984.

11. B.R. Pelly and P. Shen, 'Power transistor for choppers and inverters', An application Review, International Rectifier, EI Segundo, California.

12. G.K. Dubey, 'Calculation of filter inductance for chopper-fed dc separately excited motor', Proc. IEEE, vol. 66 No. 12, pp 1671-73, Dec. 1978.

13. B.H. Khan and S.R. Doradla, 'Comparative study of AC to DC converters employing pulsewidth modulation, International

Conference on Computers, system and signal processing, Bangalore, India, Dec. 9-12, pp. 645-650, 1984.

14. S.R. Doradla, C. Nagmani and Subhankar Sanyal, 'A sinusoidal pulse width modulated three phase ac to dc converter-fed dc motor drive', Conf. Records, Annual Meeting of IEEE Ind. Appl. Soc., pp. 668, 1984.

15. A.M., J.R and B.K. Bose, 'Three phase AC power control using power transistors', IEEE Trans. I.A., vol. IA-12, No.3, 1976.

16. E. Destobbeleer, G. Seguier, A. Castelain, 'AC-DC converter minimizing induced harmonics in industrial power system', A laboratory Applications des Redresseurs dc Puissance et Maclines Electriques - LIER d' IEEA, Universite de Lille 1, France.

APPENDIX A

Details of dc separately excited motor used :

Rated Voltage	220V
Rated Current	5A
Rated Speed	1500 RPM
Armature Resistance	4.78 ohms
Armature Inductance	0.055 H
Back emf Constant	1.46
Torque Constant	1.46

APPENDIX B

Details of components used in EPWM ac-dc converters :

	MJ10009
Transistors T_1-T_6	V_{CEV} = 600V, I_C = 20, I_{CM} = 30 A
	P_D = 175 W, For resistive load-
	Delay time t_d = 0.25 μsec
	Rise time t_r = 1.5 μsec
	Storage time t_s = 2.0 μsec
	Fall time t_f = 0.6 μsec.
Diode D_1-D_7	12SM15
Filtering inductance L	11.2mH, SWG16 iron cored
Filtering Capacitance C	50μF, 450V